การจำลองพลศาสตร์ของไหลเชิงคำนวณเพื่อขยายขนาดถังกวนสำหรับสารละลายน้ำมัน-น้ำ

นางสาวนันทิกานต์ ลมัยพันธ์

วิทยานิพนธ์นี้เป็นส่วนหนึ่งของการศึกษาตามหลักสูตรปริญญาวิศวกรรมศาสตรมหาบัณฑิต
สาขาวิชาวิศวกรรมเคมี ภาควิชาวิศวกรรมเคมี
คณะวิศวกรรมศาสตร์ จุฬาลงกรณ์มหาวิทยาลัย
ปีการศึกษา 2556
ลิขสิทธิ์ของจุฬาลงกรณ์มหาวิทยาลัย

COMPUTATIONAL FLUID DYNAMIC MODELING FOR SCALING UP STIRRED TANK

OF OIL-WATER SOLUTION

Miss Nantikan Lamaipan

A Thesis Submitted in Partial Fulfillment of the Requirements

for the Degree of Master of Science Program in Chemical Engineering

Department of Chemical Engineering

Faculty of Engineering

Chulalongkorn University

Academic Year 2013

Thesis Title   COMPUTATIONAL FLUID DYNAMIC MODELING FOR

                      SCALING UP STIRRED TANK OF OIL-WATER SOLUTION

By   Miss Nantikan Lamaipan

Field of Study   Chemical Engineering

Thesis Advisor   Pimporn Ponpesh, Ph.D.

Thesis Co-advisor   Associate Professor Seeroong Prichanont, Ph.D.

Accepted by the Faculty of Engineering, Chulalongkorn University in Partial Fulfillment of the Requirements for the Master's Degree

....Dean of the Faculty of Engineering

(Professor Bundhit Eua-Arporn, Ph.D.)

THESIS COMMITTEE

....Chairman

(Associate Professor Artiwan Shotipruk, Ph.D.)

....Thesis Advisor

(Pimporn Ponpesh, Ph.D.)

....Thesis Co-advisor

(Associate Professor Seeroong Prichanont, Ph.D.)

....Examiner

(Assistant Professor Benjapon Chalermsinsuwan, Ph.D.)

....External Examiner

(Santi Wattananusorn, Dr.-Ing.)

นันทิกานต์ ลมัยพันธ์ : การจำลองพลศาสตร์ของไหลเชิงคำนวณเพื่อขยายขนาดถังกวน สำหรับสารละลายน้ำมัน-น้ำ (COMPUTATIONAL FLUID DYNAMIC MODELING FOR SCALING UP STIRRED TANK OF OIL-WATER SOLUTION) อ.ที่ปรึกษา วิทยานิพนธ์หลัก: ดร.พิมพ์พร พลเพชร อ.ที่ปรึกษาวิทยานิพนธ์ร่วม: รศ.ดร.สีรุ้ง ปรีชานนท์, 86 หน้า.

ถังกวนสำหรับการผลิตสารเคลือบผิวผลไม้เชลแล็ก-คาร์นูบาแว็กซ์ในขั้นตอนการผสม สารละลายคาร์นูบาซึ่งเป็นขั้นตอนสำคัญที่สุดของการผลิต ได้ถูกนำมาศึกษาด้วยการจำลอง พลศาสตร์ของไหลเชิงคำนวณ ระบบในห้องปฏิบัติการประกอบด้วยถังกวนสำหรับการเตรียม สารละลายคาร์นูบา ขนาดเส้นผ่านศูนย์กลาง 220 มิลลิเมตร ติดตั้งใบพัดชนิด 6 ใบ ขนาดเส้นผ่าน ศูนย์กลาง 29 มิลลิเมตร ห่างจากผนังถังกวน 44 มิลลิเมตร และ ห่างจากก้นถัง11.4 มิลลิเมตร ใน งานวิจัยนี้เพื่อวัตถุประสงค์สองประการ ประการแรกเพื่อต้องการสร้างแบบจำลองที่นำไปใช้ใน การศึกษาพลศาสตร์ของไหลภายในถังกวนสำหรับสารละลายคาร์นูบา ผลการทดลองเพื่อหาค่า กำลังไฟฟ้าถูกนำมาใช้เพื่อสอบเทียบผลการจำลอง โดยการเปรียบเทียบจากกราฟความสัมพันธ์ ระหว่าง Power number (N_p) และ ความเร็วรอบการปั่นกวน สำหรับการศึกษาด้วยวิธีการจำลอง การปั่นกวนแบบราบเรียบในรูปแบบสามมิติร่วมกับเทคนิค Moving Reference Frame ถูกนำมาใช้ โดยแบบจำลองที่นำมาศึกษานั้นมีสองชนิด คือแบบจำลองหนึ่งเฟส และแบบจำลองหลายเฟส พบว่าแบบจำลองชนิดหนึ่งเฟสมีความเหมาะสมเนื่องจากผลการคำนวณคาดคะเนผลการทดลองได้ อย่างแม่นยำและใช้เวลาในการคำนวณน้อยกว่าแบบจำลองชนิดสองเฟส และวัตถุประสงค์ประการ ที่สองนั้น แบบจำลองชนิดหนึ่งเฟสถูกนำมาใช้เพื่อศึกษาปัจจัยที่มีต่อพฤติกรรมการไหลภายในถัง กวน ได้แก่ความเร็วรอบใบพัด ความหนืดเชิงจลน์ของของไหล และความเค้นเฉือนพบว่า การเพิ่ม ความเร็วรอบ, การลดความหนืดเชิงจลน์ และการเพิ่มความเค้นเฉือนมีผลทำให้ประสิทธิภาพการ ปั่นกวนดีขึ้น และขนาดอนุภาคของสารละลายลดลง และวัตถุประสงค์ประการที่สาม แบบจำลองที่ ได้นั้นถูกนำไปใช้เพื่อเป็นแนวทางในการหาตัวแปรขยายขนาดสเกลของถังกวนจากระดับ ห้องปฏิบัติการเป็นขนาดอุตสาหกรรม

ภาควิชา	วิศวกรรมเคมี	ลายมือชื่อนิสิต
สาขาวิชา	วิศวกรรมเคมี	ลายมือชื่อ อ.ที่ปรึกษาวิทยานิพนธ์หลัก
ปีการศึกษา	2556	ลายมือชื่อ อ.ที่ปรึกษาวิทยานิพนธ์ร่วม

5470508821: MAJOR CHEMICAL ENGINEERING

KEYWORDS: COMPUTATIONAL FLUID DYNAMICS / MIXING TANK / SCALE UP

NANTIKAN LAMAIPAN: COMPUTATIONAL FLUID DYNAMIC MODELING FOR SCALING UP STIRRED TANK OF OIL-WATER SOLUTION. ADVISOR: PIMPORN PONPESH, Ph.D., CO-ADVISOR: ASSOC. PROF. SEEROONG PRICHANONT, Ph.D., 86 pp.

A mixing tank in the critical stage of production process of shellac-carnauba wax fruit coating solution has been simulated using Computational Fluid Dynamics (CFD) technique. The laboratory system consisted of carnauba solution prepared in a lab-scale tank with 220 mm diameter (T). A 6-blade impeller with 29 mm diameter (D) was equipped at 44 mm clearance from the tank wall (off-center) and 11.4 mm from the bottom. The first objective of the research was to develop a suitable CFD model to analyze fluid dynamic of carnauba solution inside the mixing tank. Power measurement was performed and the power curve (power number versus impeller speed) was generated for model validation. The laminar mixing was simulated using three-dimensional, Moving Reference Frame (MRF) model. The model was applied based on single phase and multiphase assumptions. The result of the single phase simulation provided reasonable agreement with the experimental data; however, it required less computational time compared to the multiphase simulation. To accomplish the second objective, the single phase model was applied to study the flow behavior and the parameters influencing the fluid dynamics such as rotational velocity, viscosity and shear stress inside the mixing tank. For the third objective, the kinematic, dynamic, and geometric similarities were analyzed for scale-up criteria predicted by the CFD model.

Department :   Chemical Engineering   Student's Signature ....

Field of Study :   Chemical Engineering   Advisor's Signature ....

Academic Year :   2013 .... Co-advisor's Signature ....

ACKNOWLEDGEMENTS

CONTENTS

LIST OF TABLES

LIST OF FIGURES

CHAPTER I

INTRODUCTION

1.1 Motivation

Thailand is an agricultural country where is one of the most abundant natural resources of tropical fruits. The country's fresh fruit production is sufficient for domestic consumption and also contributes to export revenue. Rambutan is one of the most important export fruits of Thailand which accounts for 2% of the total fresh fruit export value [1]. According to the data from the Office of Agricultural Economics, the fresh rambutan export in 2012 was 165 million baht. In 2011, the export quantity was approximately 7,800 ton which increased to 12,000 ton in 2012. The growing tendency of export value has continuously increased as shown in Figure 1.1.
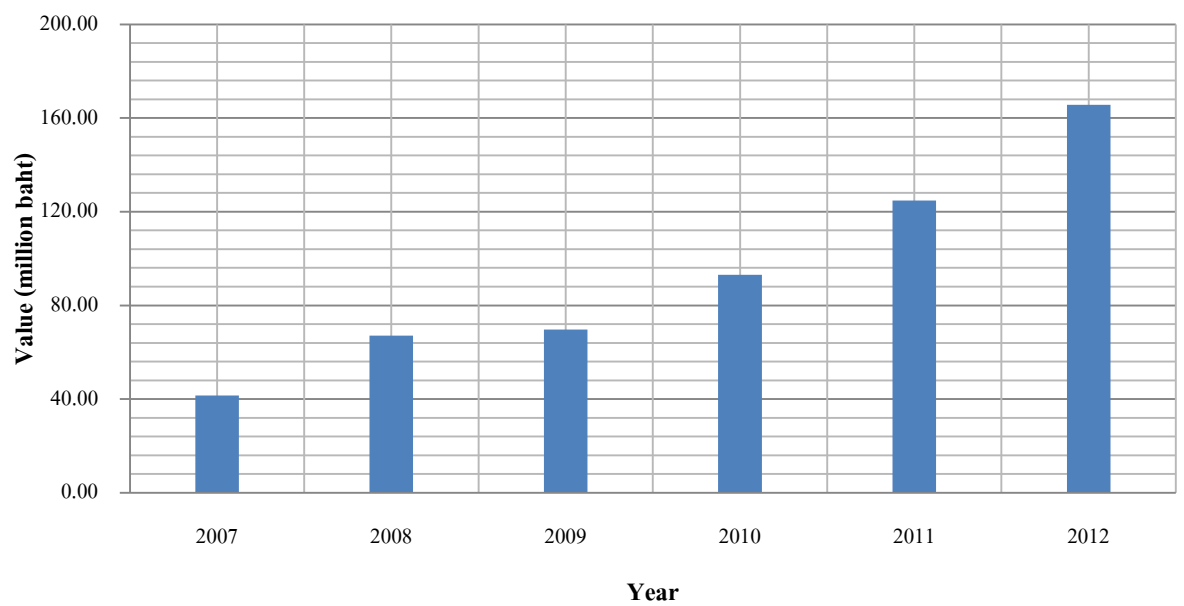
Figure 1.1 The export value of fresh rambutan between 2007-2012.

However the fresh rambutan export has been limited because the period time during transportation affects their qualities. Due to their physiologies are so plenty of spinterns all over the peel that they loss water easier after harvest. These conditions cause the problems of wither, pericarp browning and quality loss. Thus, the fresh rumbutan shelf-life is short. It is able to stay marketable for only 3 to 4 days at room temperature (25°C - 30°C). This is one reason why the trade market is still available in particular neighboring countries. Accordingly, the Ministry of Agricultural and Cooperatives established the standard principle for rambutans to ensure the acceptance qualities for the national and international level [2] such as the rambutans must be: fresh in appearance, normal smell and taste. Then postharvest handling for example: packing in storage bags or coating with wax emulsion [3] is essential.

Coating solution is one of the postharvest techniques, which is applied to fresh fruit surfaces to prevent losses (i.e. shrinking, browning, spoilage) and also to extend the shelf-life. The main compositions of the coating solution are wax, solvents and surfactant or emulsifier. Coated fruits have slower respiration rate and less weight loss than uncoated fruits [4]. Wax also helps maintain fresh appearance [5-7]. There are various types and formulas of coating solutions. The advantage of each wax is mixed to be suitable for each type e.g. physical property of those fruits. There have been the various studies for formula of rambutan coating solution. Sakulwong et al. [4] investigated shellac and carnauba wax-based formula for rambutans combined with composite plastic bags for additional handling. The results revealed the effectiveness of the formula to reduce darkening, browning and weight loss for at least 2 weeks at about 12°C. Furthermore, the treated rambutans still had normal flavors.

The formula was successfully produced in lab scale. Nonetheless, the extending of production in 30-liter tank encountered the difficulties of performing and taking time to complete homogenous solution. The increasing particle size was generated due to insufficient impeller speed during mixing and/or rate of decreasing temperature of two solutions may cause small particle formation. The small particle collected after mixing was as shown in Figure 1.2

Figure 1.2 The particle size of shellac‑carnauba wax solution increased after mixing.

The mixing process, studying of flow fields in the mixing tank, and rotating speed and pattern of the impeller are crucial for equipment design, system scale‑up, troubleshooting process and product quality control. Such studies in pilot‑scale experiments are require obvious costs and time. Moreover, industrial scale must operate several functions simultaneously [2] (dispersion, reaction and heat transfer) which do not scale up in the same time. To switch between different sizes of scale, the principles of mixing scale‑up and scale‑down, i.e. geometric similarity and dimensionless group are applied. Important characteristics such as Reynolds number, Power number and impeller tip speed should be consistent [2, 8]. However, it's impossible to keep all parameters constant. The most important parameter must be selected [9]. Even though laboratory experiments are built to investigate the suitable correlations or process parameters for scale‑up to pilot scale process, they are not always sufficient to ensure the operating conditions [10]. Scaling up the mixing of fruit coating solution from the lab scale to the pilot scale has not been successful according to the investigation by Sakulwong et al. To achieve scaling up subject, adequate experiments are required to determine the scale‑up procedure. In case of complex and costly experiment, an alternative method is to solve the balance equations numerically so that its results clarify the fluid dynamics behavior and mixing processes.

There has been an increasing interest in Computational Fluid Dynamics (CFD) for the study of fluid flow in stirred tanks. Such studies have been reported in the published literature since the 1980s [11]. CFD technology has been widely used for the simulation of mixing in stirred tanks [2, 10-13]. The CFD is a useful tool to study flow behaviors such as flow pattern, power consumption, mixing mechanism etc. [14, 15] which are macro mixing performance. The macro mixing performance is one of the most interesting subject for scale-up because it affects general mixing characteristics such as mass transfer in the tank [2]. Moreover, CFD is employed to analyze the scale up processes, in order to decrease the risk of any uncertainties in the new process [16] and minimize the expense and time consuming from experiments [17]. CFD modeling has been successfully used to study for scaling up of a laboratory experiment to a pilot process [2, 18]. However many CFD simulation studies have focused on stirred tanks of which standard impellers are located at the center. A stirred tank with a unique and off-centered impeller has been applied in the mixing process of shellac-carnauba wax coating solution because circulatory flow and swirling can be prevented. In addition, it also eliminates the need for baffles so that product hang-up on the baffle and thus, cleaning can be avoided. Such configuration will present a challenge to demonstrate its behavior. CFD method is useful to predict flow pattern in such complex configurations including hydrodynamic detailed of throughout the entire tank. Furthermore, carnauba wax derived from vegetable wax will be firstly introduced in CFD modeling.

In this research, the critical stage [19] in the production process of shellac-carnauba wax fruit coating solution, i.e. the mixing process of carnauba solution, has been studied using CFD simulation combined with the experimental data. The carnauba solution consisted of melted carnauba wax mixed with pre-wax solution, i.e. de-ionized water, 25% ammonia solution and oleic acid, at $85^{\circ}C$ will be an important part of the research. As a result, the solution prepared this step in large-scale tank will not be mixed homogeneously with shellac solution because of insufficient impeller speed during mixing and/or rate of decreasing temperature of two solutions. .

This thesis partially brought the cause from impeller speed which influence on mixing performance to examine. Also, some scale-up criteria are summarized. However, the optimum condition in lab scale has not been elucidated in this research.

A laboratory-scale process in a 5-liter tank with a 6-blade impeller will be performed for an initial validation of the CFD model. The results on power required to rotate the impeller at various speeds will be measured for the validation.

1.2   Objective of the research

1.2.1   To develop a suitable CFD model for analyze fluid dynamic of carnauba solution inside the mixing tank.

1.2.2   To study the phenomena of fluid mixing using the validated CFD model.

1.2.3   To summarize and guide the scale-up criteria for carnauba solution tank.

1.3   Scope of the research

1.3.1   Develop a suitable CFD model of carnauba solution mixing in the lab-scale mixing tank.

1.3.2   Validate the model by comparing the power number estimated as a function of impeller speed from the simulations with measured values from the experiments.

1.3.3   Apply the validated model to carnauba solution mixing in a large-scale mixing tank.

1.3.4   Suggest a scale-up criterion for maintaining similar flow pattern between small- and large-scale mixing tank.

1.4   Benefits of the research

1.4.1   To obtain suitable model for mixing behavior inside a mixing tank with off-center impeller.

1.4.2   To elucidate the transport phenomena in a mixing tank using the CFD model.

1.4.3   To suggest a guideline scale-up criteria which are suitable for carnauba solution tank.

CHAPTER II

THOERY AND LITERATURE REVIEWS

2.1 Fruit coating production process development of shellac- carnauba wax based

Since Sakulwong et al. [4] successfully investigated shellac and carnauba wax-based formula for rambutans by dipping method, this treatment helped maintain rambutan quality for at least 2 weeks at about 12°C when combined with composite plastic bags. Figure 2.1 showed shellac and carnauba wax based for dipping rambutan. Then, expanding the production capacity in a laboratory to an industrial scale was attempted. They confronted the difficulties of performing, taking long time and increased particle as discussed in previous section.

Figure 2.1 Shellac and carnauba wax based for dipping rambutan.

Thereafter, Nirotanan et al. [19] developed the production process of shellac and carnauba wax based of Sakulwong et al. method [20] to be simpler and more effective. The wax coating solution was prepared by melting the carnauba wax at 85°C before adding with pre-wax solution (which consisted of de-ionized water, 25% ammonia solution and oleic acid) at the same temperature so that it was easier to be mixed. Then, the carnauba solution was gradually added in shellac solution at 60°C. They investigated that the impeller speed of 180 rpm was sufficient to generated homogenous solution. The particle size of the final solution was in the range between

7.96 µm to 16.76 µm. At lower of that speed, they found that the solution would be not homogenous after mixed carnauba solution in shellac solution. Thus the impeller speed was major criteria of mixing efficiency. However scale up ambition have been still required to be achieved.

2.2   Fluid Mixing

2.2.1   Studies on mixing

The study of non-reacting, turbulent fluid mixing can be divided into three aspects, the gross scale, fine scale and turbulence energy spectra.

Gross scale study is relating to the overall flow pattern in the tank. This study can give qualitative and quantitative information which is useful of primary selection of impeller type and design parameter in system.

Fine scale study base on three different theories; direct numerical simulations (DNS), large eddy simulation (LES), and the Reynolds averaged Navier-Stokes (RANS) approach. This method still requires the computational technique.

Turbulence Energy spectra studies the various velocity fluctuation in order to determine the turbulent energy spectrum, $E(k)$ including turbulence length scale.

2.2.2   Impeller type

In mixing application, impeller is an essential tool as it produces flow and shear to fluid [21]. That is to say, when impeller is rotating, it transports the kinetic energy from the blades to the surrounding fluid. Generally, the purposes of impeller i.e. producing flow or shear depend on mixing application. In application of blending the liquid and solid suspension is more required impeller generated mass flow while reacting application is more required impeller which generates shear.

Impeller type also can be classified into two types as it circulates fluid axially or radially so that impeller is conveniently divided according to which these flow direction is important.

a)   b)
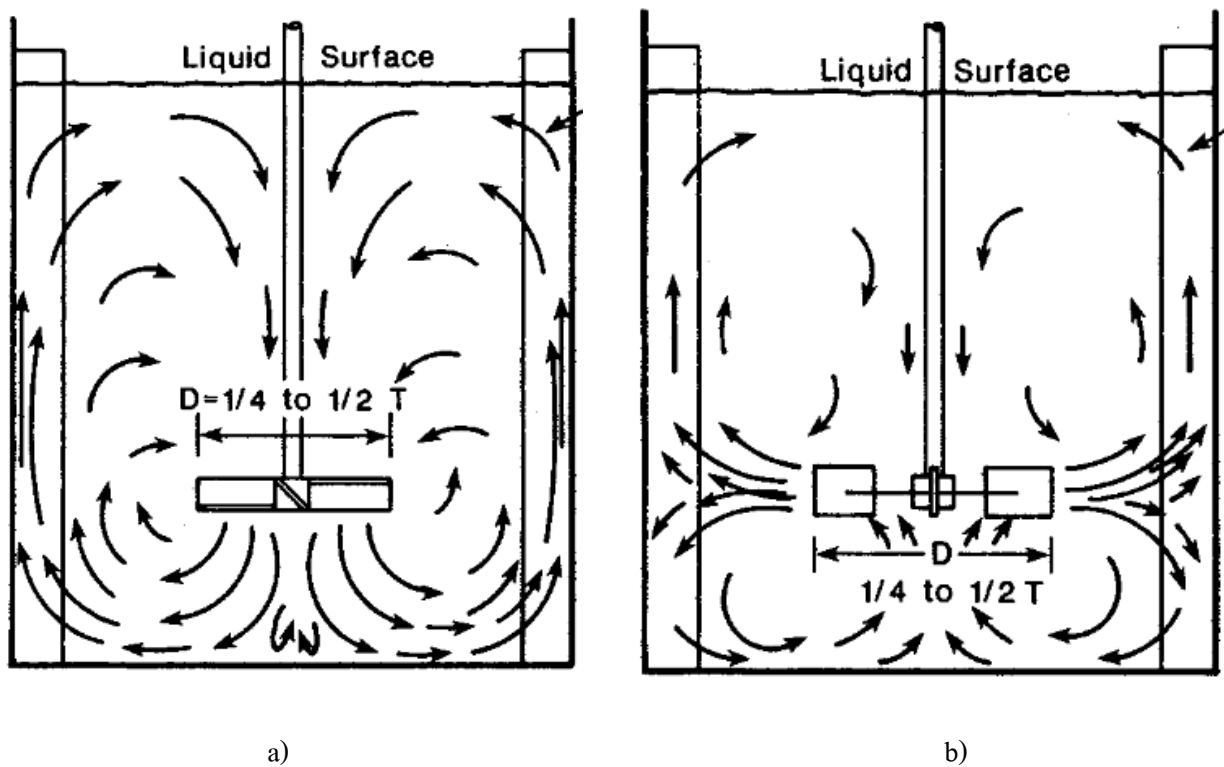
Figure 2.2 Flow pattern of different impeller type .

a) Flow pattern for axial impeller,   b) Flow pattern for radial impeller

2.2.3   Mixing application

Laminar and turbulent mixing plays an important role in chemical engineering application. In mixing process, species transports on different length scales. Convection is considered on large scales, while diffusion is analyzed on molecular scales.

Some example applications of laminar mixing are high-viscosity materials in food industries [22-24] and manufacture of lubricant [25], the production of cosmetics such as creams and unguents, the mixing of detergents and the agitation of shear-sensitive cell in biopharmaceutical industries [26, 27].

Mario et. al [28] studied the performance of eccentric impeller in laminar stirred tanks using tracer visualization technique and laser induced fluorescence (LIF). The working fluids of the experiment were mixture of glycerin and water (Re = 12.5-50.0). From the result they proposed the mixing performance to eliminate unstable manifolds which can be avoid damage

generated by mechanical stress such as mammalian cell culture and biotechnological application. However, in conclusion they suggested that three-dimensional comprehensive of mixing mechanisms should be further studied which computational technique is required.

2.3   Scale-up and scale-down of liquid mixing system

When system geometry is changed, the physical and mechanical variables such as chemical environment in the tank will not be constant. Therefore, the productive quality has been changed. There is no universal method which is employed in scale translation. Many methods have been proposed depending on the mixing purposes. There have been different factors affected the particularly processes. The basis of scale-up or scale-down principles is the similarity and dimensionless groups [8]. The criteria for similarities are expressed in term of the geometrical similarities among different sizes of equipments such as shape and of the force ratio of corresponding dimensions are maintained. Global scaling dimensionless analysis such as Reynolds number, power number and Froude number were proposed in published literature by Nagata et al. [8].

CFD method has been widely used to analyze the system in experimental scale before scaling up for pilot scale. Li et al. [2, 10, 17, ,18, 29, 30] applied CFD for scale-up study by comparing macro mixing performance such as power number, flow number, secondary flow number and pumping efficiency in various laboratory scale tanks. The results of those parameters had been slightly changed so the operating condition of pilot-scale can be chosen. However, micro mixing performance study was their next step work. In this same method, Compolo et al. [10] used CFD to investigate the power and impeller speed for various operating conditions, they successfully found the operating conditions which ensured the optimum fluid dynamic efficiency. Moreover, Alexopoulos et al. [17] developed CFD to compared the micro mixing performance such as energy dissipation rate in a scale-up reactor, the result showed agreement of the small-scale and large-scale. Obviously, such method has no scaling up or scaling down problems because it solves the fluid dynamic equations in the same phenomena as mention by Jayanti et al. [31]. However, the physical phenomena are still required.

2.3.1   Reynolds number

Reynolds number (Re) is a ratio of inertia and viscous forces. The Reynolds number (Re) is the dimensionless number which describes the hydrodynamic in the system. It provides a criterion for dynamic similarity [9]. The Reynolds number (Re) is defined as

$$\text{Re} = \frac{\rho N D^2}{\mu} \qquad (1)$$

Where
ρ = density of fluid (kg/m^3),

N = Impeller speed (Revolutions per second, rps),

D = Outer diameter of impeller (m),

μ = Viscosity of fluid (kg/m-s).

2.3.2   Froude number

The Froude number (Fr) represents the number which accounts for vortex formation occurs and effects in the system. It describes the ratio of inertial to gravitational forces.

The Froude number (Fr) is defined as

$$Fr = \frac{DN^2}{g} \qquad (2)$$

Where
N = Impeller speed (Revolutions per second, rps),

D = Outer diameter of impeller (m),

g = Gravity force (m/s^2)

2.3.3   Impeller tip speed

The impeller tip speed (V_{tip}) is defined as

$$V_{tip} = \pi ND \qquad [\text{m/s}] \qquad (3)$$

Where   N   = Impeller speed (Revolutions per second, rps),

D   = Outer diameter of impeller (m).

Impeller tip speed (V_{tip}) is related to the geometry and the agitation rate of mixing tank [32].

2.4 CFD model of mixing process

CFD modeling was one approach of studies involving in mixing mechanism : molecular, eddy and bulk (convection) [33] which was proposed to be realistic method. The models necessary for the laminar mixing included impeller models or/and multiphase model. This section summarized the CFD model relating to our thesis. Details were discussed as follows:

2.4.1 Impeller modeling

Impeller played a fundamental role in mixing process, since it was a crucial tool to determine production quality. The approaches commonly used for modeling of rotating impeller, were multiple reference frame (MRF) and sliding mesh (SM). Both of them divided solution domain into two regions; inner region which rotated with the impeller and outer region which was stationary. The flow with rotating reference frame models was defined as Figure 2.3 [34]. The interface between two reference frames (dashes line) was assumed to be stationary flow. The MRF model was applicable for a steady flow and for a system with weak impeller-baffle interaction. Conversely SM model was used for an unsteady which unsteady interaction was not able to be neglected i.e. when the impeller-baffle interaction is strong. In case of time-dependent system, SM model calculated the phenomena of the impeller rotation more accurately, but had high computational expense [11, 35].
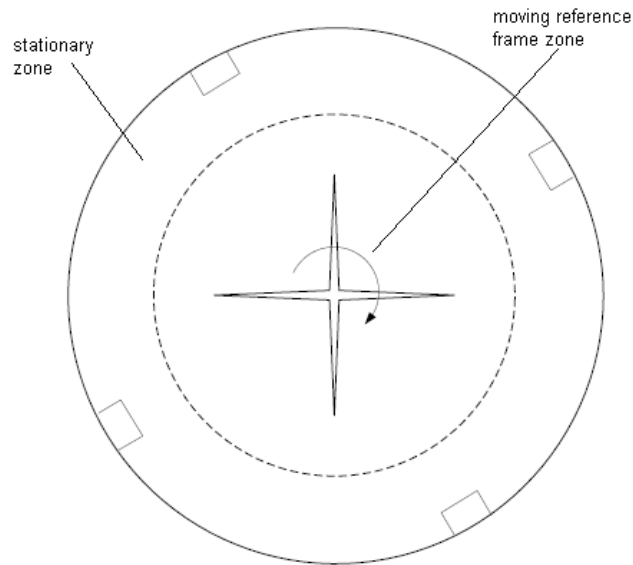
Figure 2.3 Domains of a rotating reference frame of single impeller.

CFD simulation of flow fields in stirred tanks have been studied by many authors [17, 36-38]. In baffled mixing tanks, simulations were mostly carried out using the SM [39] which were suitable for mixing with the interaction between impeller and baffle. In case of unbaffled vessels, the simulations have been suitably performed using MRF where the impeller was assumed to be stationary and the reference frame or coordinated system was rotated. As a result of it was easy to define the outer-wall boundary condition [17, 40].

Deglon et al. [41] demonstrated CFD simulation for six-blade Rushton turbine impeller in baffled tank which the system was consisted of 25°C water by using MRF model and the standard k-ε model (i.e. the turbulence model). Higher-order discretization scheme with very fine grids was applied. They minimized the computational demand by using the pseudo-steady state MRF impeller rotational model. It was shown that the simulated results by the MRF model were similar to those by the SM impeller rotation model for steady-state stirred tanks.

Consequently, in this research, both of MRF and SM can be applied. Nevertheless, SM model consumes more computational time.

2.4.2   Multiphase model

Accordingly multiphase flow was widely present in variety of chemical engineering application. Its particular flow regime comprehensive was important. The use of multiphase flow modeling of CFD simulation was extensively applied. However there was no universal multiphase model could be applied for all regimes. The selection of appropriate multiphase flow model CFD for such flow was prior because it determined the ability to accurately prediction of the realistic behavior of the fluid flow. At present CFD simulation provides several type of multiphase flow model according to their level of complexity. These example type were summarized as follows in Table 2.1 [42].

Model	Description	Flow regime
Eulerian Model	- Continuity, momentum and (optionally) energy equations are solved for each phase.	- Slurry flow - Fluidized bed - Droplet flow
Mixture Model	- Simplified from Eulerian approach - Solved the continuity, momentum and energy equations for the mixture. - Allow the phases to be interpenetrating.	- droplet - bubble - slurry flow
Volume Of Fluid (VOF) Model	- Tracked location and motion of the interface between phases - Two or more fluids (or phase) are not interpenetrating. - Solved the continuity, momentum and energy equations by sharing velocity among the phases.	- slug flow - free surface flow

Table 2.1 The various types of multiphase flow model

2.4.3   Model validation

To evaluate the CFD model, the simulation results were compared with the experimental data. An extensive number of literatures [10, 11, 43, 44] used power number to validate the simulation, due to power number is proven to be a reliable predictor. Marina et al. [10] informed that they chose this parameter because of three reasons: it's indicative parameter of complex three dimensional turbulent flow; it's normally available by industries: and it can be easily measured.

The dimensionless power number (N_p) was defined as

$$N_p = \frac{P}{\rho N^3 D^5} \cdot$$

(4)

Where   P   = Power the impeller (Watt),

ρ = Density of fluid (kg/m^3),

N   = Impeller speed (Revolutions per second, rps),

D   = Outer diameter of impeller (m).

The power can be measured through the total torque (Γ), m-blade impeller was calculated by

$$P = 2\pi m N \Gamma.$$

(5)

The total torque required to rotate the impeller which can be calculated from summation of pressure differential between the front and the back on each blade at surface element i, A_i is area of the surface element i and r_i is radial distance from axis of shaft on the position which impeller is equipped [31] .

$$\Gamma = \sum_i (\Delta P)_i A_i r_i$$

(6)

The Reynolds number (Re) was defined in Equation (1)

The data of power number and Reynolds number obtained from varying impeller speed was then plotted as general energy curve or power curve on log-log plot. It illustrated the relationship between power number and Reynolds number of unique system.
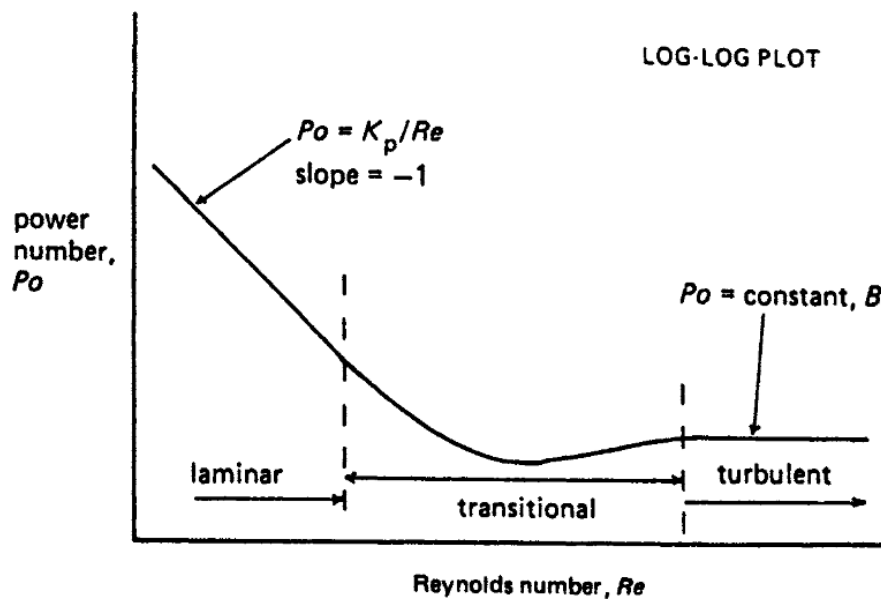
Figure 2.3 A typical power curve [45].

Figure 2.2 showed the general power curve, it depicted that it consisted of three regions of the mixing.

At low Reynolds number, the flow was in laminar regime in which the mixing initially and slowly occurred. The blending was carried out by the velocity distribution without turbulent dispersion. Consequently, the effects of molecular diffusion were very slow. In this region, power number was decreased corresponding to Reynolds number [45].

At higher Reynolds number, the flow was turbulent. The velocity distribution eventually generated interfacial area between components. In this region, the fluid was rapidly mixing as a result of turbulent eddies were present. Thus, molecular diffusion effects in fluid were faster. In turbulent region, power number was constant.

In the region between laminar and turbulent flow was transition region. However, this region had no simple mathematic relationship between power number and Reynolds number.

Among power number - Reynolds number plot, each type of impeller including its environment has its own particular shape of curve as shown in Figure 2.4.
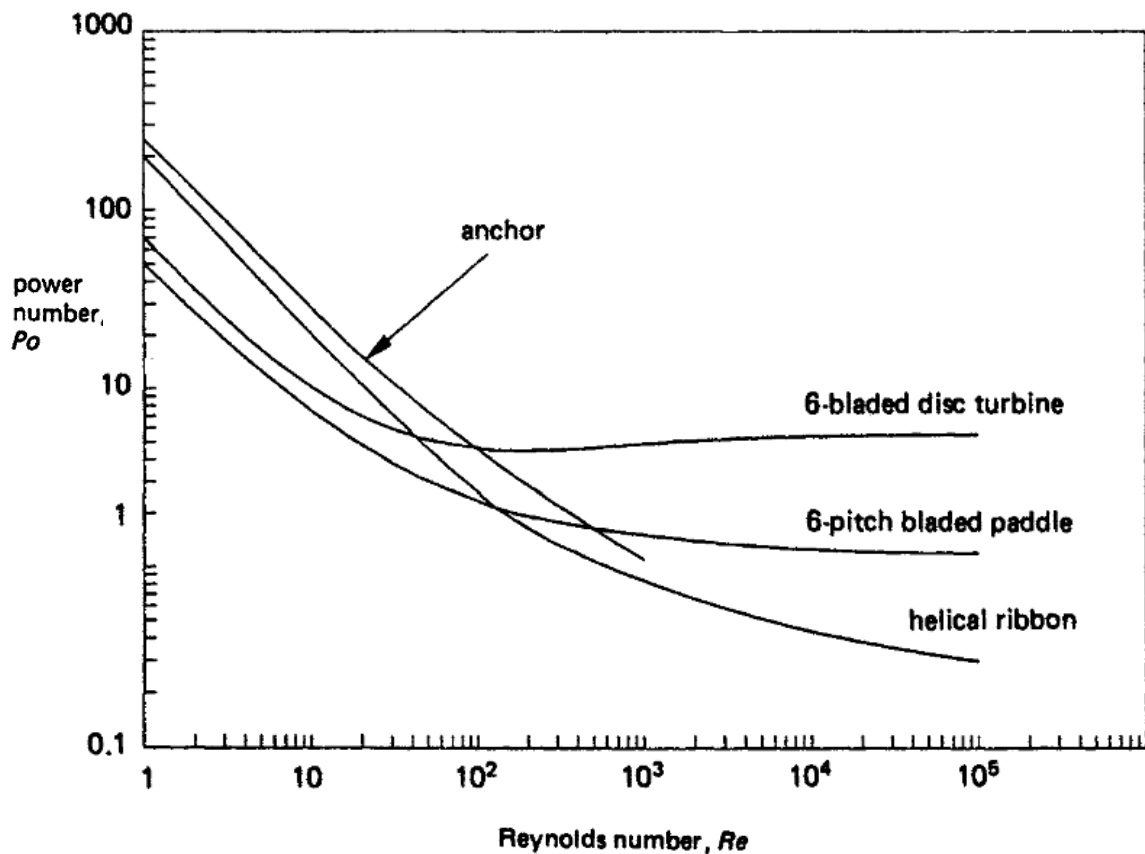
Figure 2.4 Power curves of different impellers [45].

2.5 Computational fluid dynamics (CFD) model of shellac-carnauba wax fruit coating solution.

Nirotanan et al. [46] used CFD modeling to scale up the mixing tank of shellac-carnauba wax fruit coating solution. In their study, the critical stage of production in a 5-liter mixing tank was simulated. Then the model was applied to calculated impeller speed to be used in 200-liter tank. Nonetheless, they still had no rigorous validation data from experiments to evaluate their model.

2.6 Computational fluid dynamics

Computational fluid dynamics (CFD) is a field of study relating fluid mechanic by means of numerical solution of conservation equations for mass, momentum and energy in flow regions of interest, couple with additional equations relating to the problems [33]. CFD is a complement approach between theory and experimental approaches. It is a powerful approach as the research and design tools. There are three main steps for CFD simulation it provides three main steps (i) a pre-processor (ii) a solver (iii) a post-processor

Pre-processor

In this step, the information such as computational domain, grid (mesh) generation, physical and chemical phenomena (i.e., governing equation), material properties, etc. is set up in CFD simulation software, Fluent (Fluent 14, ANSYS Inc., Lebanon, NH., USA).

Solver

The second step, after the meshes have been read into the solver, the partial differential equations (based on Navier-Stokes) are discretised over the meshes [33]. Boundary and initial conditions are defined to CFD. Then, a large set of nonlinear simultaneous equations is produced. To solve these, there are three distinct streams of numerical solution discretisation, including finite difference, finite element and finite volume methods. Generally, the solver performs the following steps:

- Approximate unknown flow variables by simple function
- Carry out in discretisation step, they transforms the PDEs into algebraic equations

Fluent is computer program for modeling fluid flows, heat transfer and chemical reactions in complex geometries. Fluent is the most widely used commercial CFD code both in industry and in academia. It is based on finite volume method. Meshes generated by other meshing software can be imported into Fluent. Fluent provides researchers with powerful tools to investigate various engineering flow problems such as incompressible or compressible flows, Newtonian or non-Newtonian flows, viscous or inviscid flows, laminar or turbulent flows, single-phase or multi-phase flows, species transport etc. in both steady-state and transient situations. Various modeling features are available to apply FLUENT to specific applications.

For an incompressible system, an independent equation to calculate pressure is absence. A pressure-velocity coupling algorithm was required to derive equations for pressure from the continuity and momentum equations. In this study, the Coupled scheme for Pressure-Linked Equations algorithm was applied. Then, Pseudo Transient was enabled as recommended by FLUENT as it helped decrease number of iterations for convergence. The PRESTO Method for Pressure-Linked Equations algorithm was applied.

Post-processor

The final step, post-processor provides full-field data such as visualization result, geometry and grid display, vector plot, line and shaded contour plots, etc. at each and every point in the domain.

2.7   Governing equations of fluid dynamic

CFD is based on fundamental physic principles of fluid dynamics

General transport equation

$$\frac{\partial(\rho\phi)}{\partial t} + \nabla \cdot (\rho\phi \mathbf{u}) = \nabla \cdot (\Gamma \nabla \cdot \phi) + S_\phi \tag{6}$$

The general balance equation over the stirred tank can be written for each system variable ø in Equation 1

1. Mass is conserved (Continuity Equation)

$$\frac{\partial \rho}{\partial t} + \nabla \cdot (\rho \mathbf{u}) = 0 \tag{7}$$

The fluid density is designated by ρ. The velocity vector ($\mathbf{u}$) of fluid is defined as

$$\mathbf{u} = u\mathbf{i} + v\mathbf{j} + w\mathbf{k}$$

For an incompressible fluid, the density of fluid (ρ) is constant, consequently continuity equation can be arranged as

$$\nabla \cdot u = 0 \qquad\qquad (8)$$

2. Newton's second law of motion (momentum equation)

$$\rho \frac{Du}{Dt} = -\nabla p + \nabla \cdot \tau + S_M \qquad\qquad (9)$$

The pressure and viscous stress of fluid are denoted by ρ and τ respectively. S_M is the momentum source term.

In this study, the flow model is based on solving Navier-Stokes equations for laminar mixing. For solving a set of nonlinear governing equations in three dimensional, CFD code (Fluent, ANSYS Inc., Lebanon, NH), a finite volume based fluid dynamic analysis program is utilized.

CHAPTER III

RESEARCH METHODOLOGY

3.1 Objective and Approach

According to the objectives of this thesis discussed previously in the introduction, the overview approaches to achieve these objectives were delineated in the flow diagram Figure 3.1.

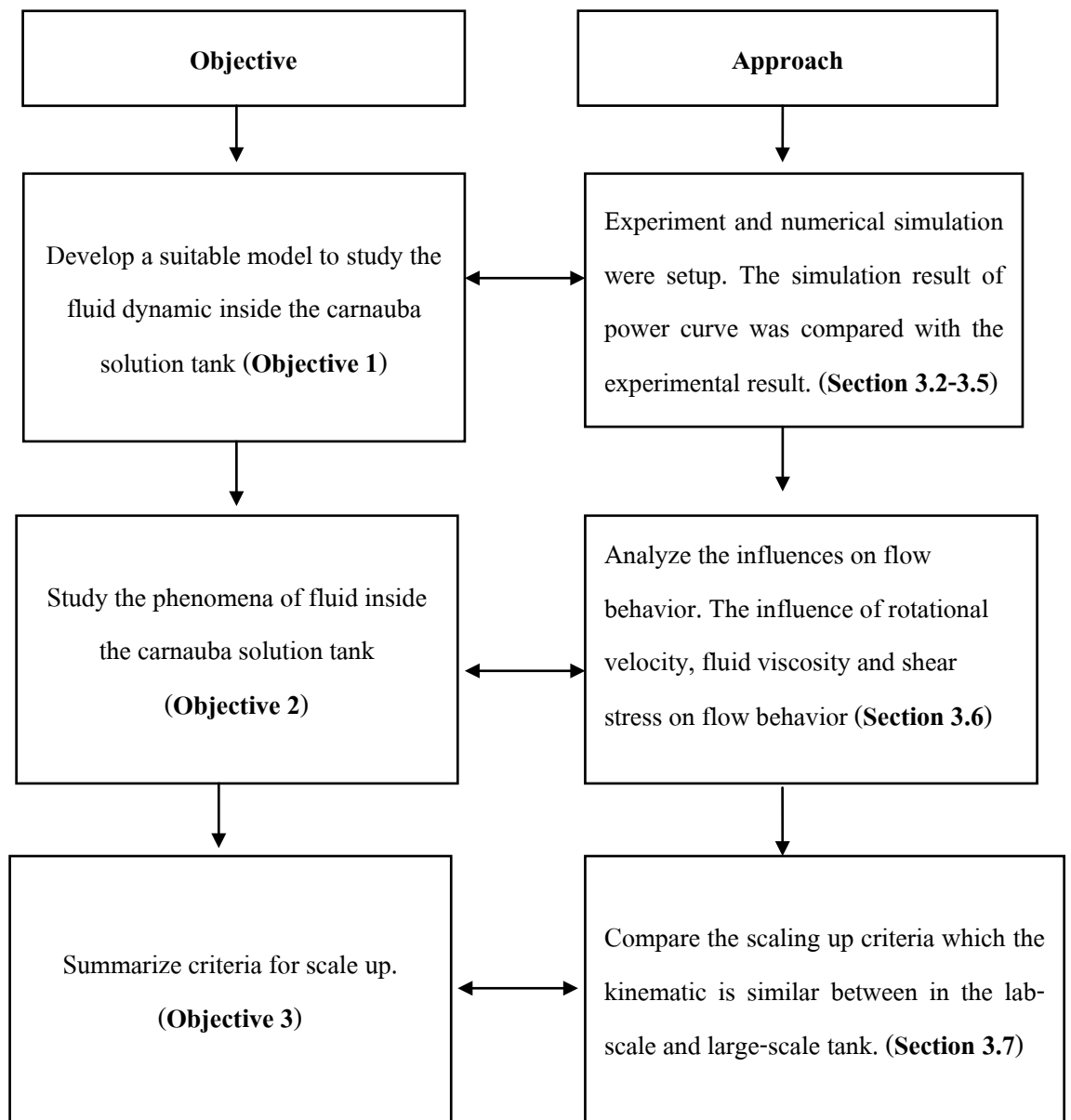| Objective	Approach
Develop a suitable model to study the fluid dynamic inside the carnauba solution tank (**Objective 1**)	Experiment and numerical simulation were setup. The simulation result of power curve was compared with the experimental result. (**Section 3.2-3.5**)
Study the phenomena of fluid inside the carnauba solution tank (**Objective 2**)	Analyze the influences on flow behavior. The influence of rotational velocity, fluid viscosity and shear stress on flow behavior (**Section 3.6**)
Summarize criteria for scale up. (**Objective 3**)	Compare the scaling up criteria which the kinematic is similar between in the lab-scale and large-scale tank. (**Section 3.7**)

Figure 3.1 The flow diagram of thesis objectives and its approaches.

A suitable CFD model of carnauba solution in a lab-scale tank which equipped with 6-blade and off-center impeller has been developed. The validated CFD model used to study the phenomena inside the mixing tank and influence of rotational velocity and fluid viscosity on flow behavior. Besides the CFD model in lab-scale will be applied in pilot-scale tank in order to guide the dimensionless criteria of scaling up.

To delve into the detail of each approach in the next sections, the procedure overview can be divided into two parts, preliminary study and carnauba solution study. Similarly, the two parts of study were conducted in 220 mm diameter (T) lab-scale mixing tank. 6-blade impeller with 29 mm diameter (D) was equipped off-center at 55 mm clearance from center and 11.44 mm clearance from bottom. The dimensions of the mixing tank, the impeller and located position were presented in Table 3.1 and Figure 3.2.

Dimension of tank and impeller (mm)	Value
Tank diameter (T)	220
Liquid height (H)	106.48
Liquid volume (V)	5 L
Impeller diameter (D)	29
Impeller clearance from tank base (C_{imp})	11.44
Impeller clearance from tank center (C_c)	55
Number of blade	6
Blade width (b)	18.93
Blade angle	60

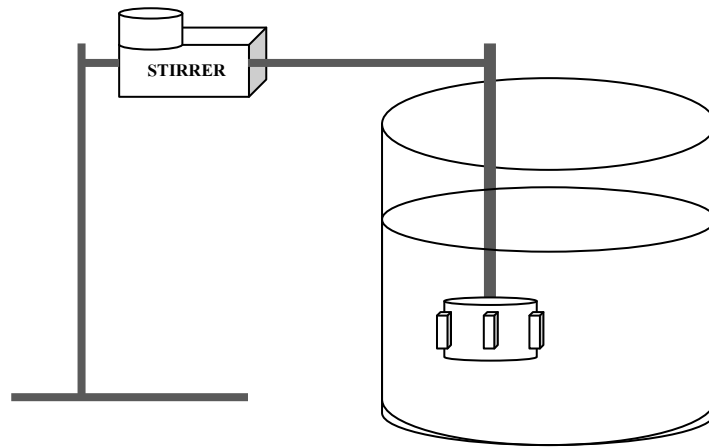**Table 3.1** Dimension of the mixing tank and impeller

Figure 3.2 Physical geometry of the mixing system and 6-blade impeller.

3.2 Preliminary Study

The purposes of a preliminary study were made in order to initialize the solution of model. The setting up boundary condition and post-processing were examined. Due to the carnauba and itself solution preparation was costly material and required time to conduct an experiment. Water was initially used instead because it was simple, less cost and fundamental fluid of most industrial application. Also, other purpose of the study was to investigate the effect involving in viscosity of fluid inside mixing tank (Objective 2 of the research). The influence of viscosity of water and carnauba on flow behavior will be compared. Procedures of this study consisted into two parts, experiment and CFD simulation.

3.2.1 Experimental Setup

The experiment was set up to obtain power of the impeller by means of electrical measurement using multi meter. Water is filled at the level of 150 mm. The data of current (amperes) were collected while water was mixing at various impeller speeds from 2000 to 2900 rpm. The constant potential difference (volts) was also measured.

Stirrer

Multi meter

Mixing tank equipped with 6-blade impeller
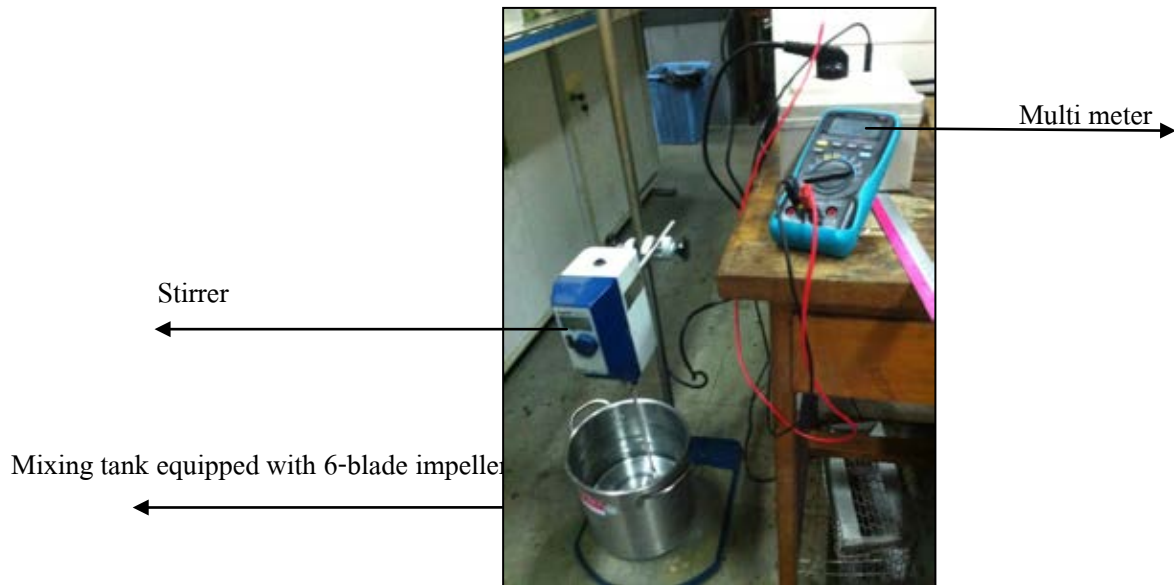
Figure 3.3 Power measurement setup of water.

The data of voltage (volts) and current (amperes) was converted into power (watt) as the equation of Ohm's law formula, [47]

$$P = IV \qquad (10)$$

Where

     P   =   Electrical power (watts),

     I   =   Current (amperes),

     V   =   potential difference (volts).

The experiment was primal procedure with the purpose of classify the flow region i.e. laminar, transition or turbulent which could be identified by power curve as discussed in the literature reviews in Figure 2.3. Since, the existed region from experiment was crucial to choose the appropriate model solution in step of simulation setup which was discussed in the next paragraph.

3.2.2   Simulation Setup

Computational simulation was carried out based on experimental setup. The transport equations were numerically solved using the commercial CFD simulation software (Fluent, ANSYS Inc., Lebanon, NH). The Microsoft Window 7 Home premium computer installed on Intel Core i7-2600 processor (3.84 GHz, 64 bit) and 8.00 GB RAM was utilized. The steps towards solving the problem were determining the geometry, meshing and initializing the solution of the model. These procedures and required information were described as follow subsections.

3.2.2.1 Geometry consideration

The geometry of the model was generated according to Table 3.1 and Figure 3.2. Figure 3.4 and 3.5 showed the comparison of actual impeller shape and computational impeller.

.

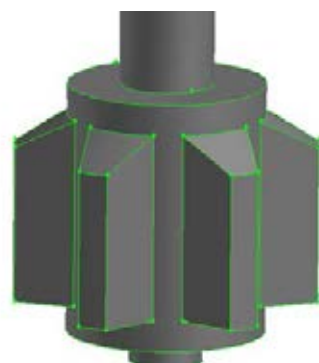**Figure 3.4** Actual impeller

Figure 3.5 Computational impeller

The computational geometry was generated in three-dimensional tank (Figure 3.6) because the impeller was placed off-center so the geometry was not able to be partial in symmetry domain. The partition technique was applied in order to be easier to generate mesh.

3.2.2.2 Mesh generation

Once the geometry was made, the computational domains were then defined. This thesis was employed the MRF technique as discussed previously in the literature reviews. Region inside the mixing tank was divided into two reference frames; the moving reference frame attached to the region near impeller motion and stationary reference frame attached to the rest region. The Figure 3.6 depicted the two reference frames inside the mixing tank by the use of the partition technique so that a structured mesh of hexahedral mesh could be create in complex geometry. The uniform structured grids were created due to its advantage of taking less time than an unstructured grid calculation. The structured meshes were applied throughout the mixing tank as shown in Figure 3.7.
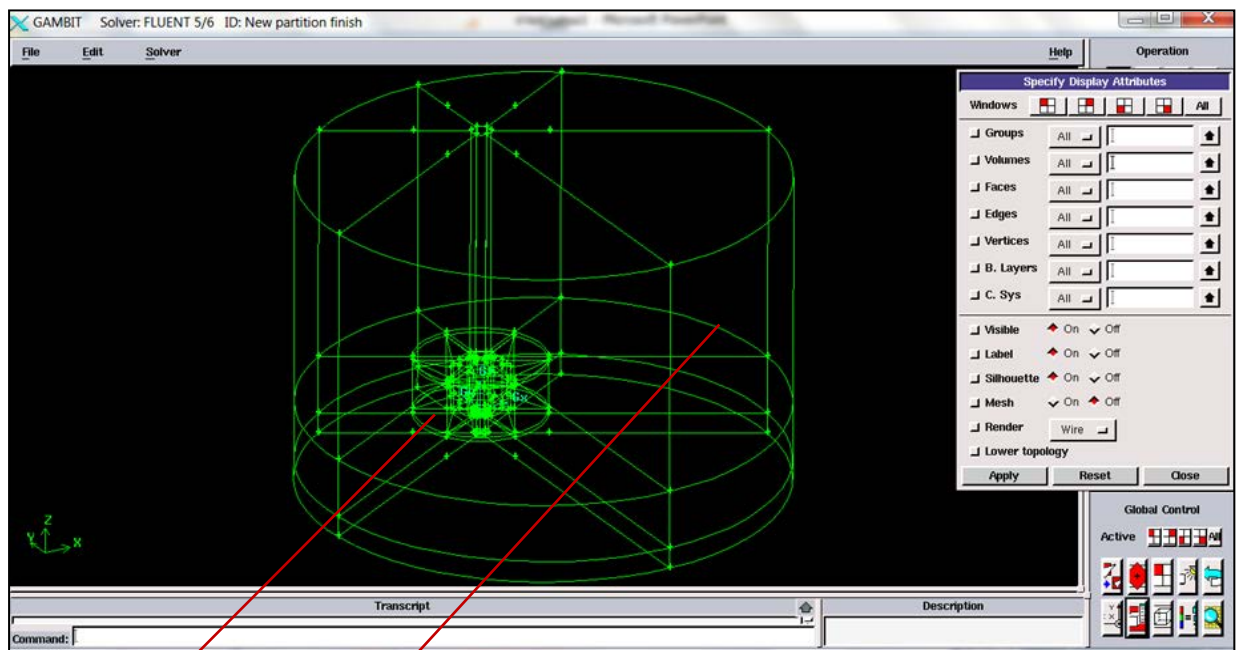
Moving reference frame Stationary reference frame

Figure 3.6 The three dimensional reference frames of the mixing tank.
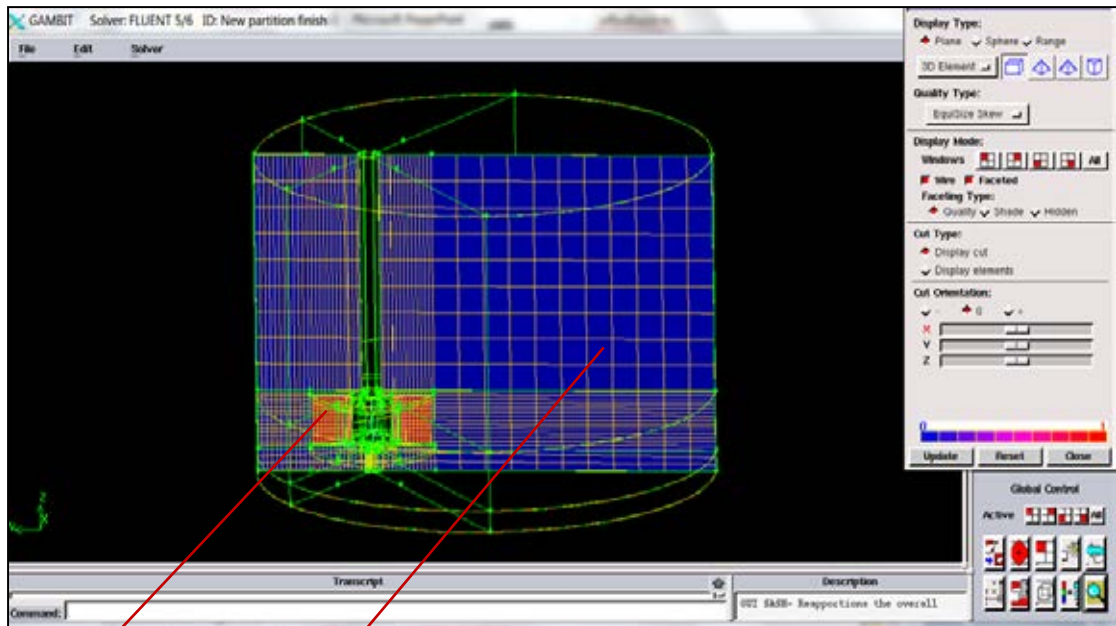
Figure 3.7 Structured mesh throughout the mixing tank

Fine mesh

Coarse mesh

Finer mesh was applied in especially better resolution in region of impeller motion in order to capture the higher velocity gradient zone. The quality of mesh was repeatedly improved by using adaptive mesh technique in grid sensitivity analysis in which will be described in section 3.6.

3.2.2.3 Model solution

After the meshed geometry was introduced into the solver, the final step was initializing solution of the model. Some assumptions were made in order to simplify the flow problem and minimize the time required for calculation.

Model assumptions are the followings:

As discussed previously that the preliminary studies was to investigate the mixing of water inside the tank. The model solution was performed in two models: single phase (water) and

multiphase model (water-air) which was based on different assumptions. Therefore **the working fluids were almost water, considered to be incompressible**.

Due to the mixing tank was insulated, there was no external source of heat transfer into the system. Thus **inside the mixing tank was isothermal system**.

This research applied MRF model with the assumption of the moving and stationary zone interactions were relatively weak so the **flow was a steady-state approximation**.

However additional different assumptions for each case of study are further discussed in an upcoming subsections.

The next subsection described the solution initialization details of single phase and multiphase model. The two models were based on different assumption. Complete specification setups of both models were in Appendix A and B.

3.2.2.1   Single phase model

The viscous model for laminar flow called single phase model was simulated in case the effect of air on the top of the mixing tank was neglected so that the system was fulfilled with water.

Parallel processing was used instead of series because of minimizing the solving time in FLUENT as reported by Hannah Duscha et.al. [48]. Pressure-density Based solver was used that it solves the equations of continuity to calculate velocities based on pressure. The solution methods were kept at default of laminar model for single phase flow.

Material for single phase simulation was pure water. The physical properties of simulated materials are shown in Table 3.2.

General specifications relating to the rotating reference frame were on Cell Zone Conditions for moving zone and stationary zone. Moving zone was set up the rotational velocity from 2000 to 2900 rpm respectively. While stationary zone was keep at default, the shaft was set as moving wall at the same rotational velocity. The other zones were kept as default because they were stationary wall.

On Reference Values, Area and Length were accounted from impeller configuration, Velocity was converted from the rotational velocity, the others i.e. Density, Pressure and Temperature were water properties.

Selecting Monitors, the pressure and velocity in a new created surface were additional monitored during solving combined with residual error monitored. Due to the default convergence criteria are not sufficient to access the correct flow feature in a mixing tank [35]. This technique helped observe the solving solution besides decreasing Residual constraints as proposed by Hannah Duscha et.al. [48]. This research applied this technique excepting for Residual monitored. The Residual of all criteria was initially enabled until $1x10^{-3}$ error criteria, then the residual monitor of all criteria was disable check. The calculation of the solution was continued in which Surface monitors of pressure and velocity maintained in place. The velocity and pressure Surfaces showed the results of solution throughout the solving process. These Surface plots helped ensure the final solution accomplished. Consequently, the trends of Area Average Weight of velocity and pressure plot were observed until they were constant.

3.2.2.2   Multiphase model

The viscous model for laminar flow solving for each water and air phase called multiphase problem was developed in case of taking into account of air in the system. This case was used because of the assumption that air affected the mixing.

General problem setup for multiphase was similar to the single phase with a few different options. The first difference was the Multiphase on Models setup. The Multiphase was turn on that consisted of three Multiphase models i.e. Volume of Fluid (VOF), Mixture and Eulerian. VOF model was chosen to dictate the interactions between the two phase of air and water because of literature and numeric recommendations [42] in which it was utilized for this type of two-phase flow and as mentioned in Chapter 2 literature reviews.

The Materials were indicated as water and air in which water was primary phase and air was secondary phase. As a result of water was considered to be continuous phase while air was dispersed phase.

The second difference, selecting Solution Method of the (Multiphase) Couple was the scheme which recommended in the Help panel of ANSYS FLUENT [35]. This method solved all equations for each phase velocity and shared pressure correction simultaneously [49]. Coupled of Pressure-Velocity coupling was proposed as it was capable in steady state and transient with large time step condition.

On boundary condition and new surfaces on Monitored were created as same as single phase setup.

The third difference, after Initializing on Solution Initialization, the primary and secondary phase zones were required. A Hex shape of on Region Adaption was created in z-Coordinate. The z-coordinated was defined the height of primary phase. Patching on Solution Initialization, water phase volume fraction was indicated.

The Courant number was kept default without changing relaxation factor.

Since the preliminary study was obtained the solution of model which the result was agreement with experiment (the detail will be discussed in the result and discussion), then the CFD model was applied to carnauba solution.

3.3 Carnuaba solution Study

The carnauba solution was an actual fluid which will be used in scale up proposal. This study was applied from preliminary study but some differences were made in order to modify model. The procedure of carnauba solution was also consisted of experiment and simulation as present followings.

3.3.1 Experimental setup

Shellac–carnauba wax fruit coating solution, the preparation step of carnauba solution prior influenced the final solution. In other word, carnauba solution step was the critical stage as mentioned in introduction. Carnauba solution consisted of percentage by volume of 81 % water, 5 % carnauba wax, 9 % ammonia and 5 % oleic acid was prepared. The carnauba wax was initially melted at 85^{0}C. Then the melted carnauba wax was eventually added in the mixture solution of

water, ammonia and oleic acid in while it was mixing at 85^0C. A thermometer was equipped in order to keep the production process at 85^0C during mixing. Then completed emulsion of carnauba solution was setup to measured power as the same method of preliminary study at impeller speeds from 2000 to 2900 rpm. Figure 3.8 shows the power measurement setup of carnauba solution.

Figure 3.8 Power measurement setup of carnauba solution.

3.3.2 Simulation setup

The simulation setting up of carnauba solution was similar carried out to preliminary study. The carnauba solution was employed both of the single phase and multiphase model for comparing the accuracy of prediction. The suitable model was chosen based on validation result in which will be discussed in the next chapter.

3.3.2.1 Single phase model

The single phase of carnauba solution was applied from preliminary study of single phase model. The procedure was similar to that simulation. Also, the assumptions were based on

preliminary study of single phase model. A few differences were made. The first difference was creating Materials. Carnauba solution property was indicated instead of water. Required carnauba solution property was shown in Table 3.2.

3.3.2.2   Multiphase model

Also, multiphase simulation of carnauba solution was developed in which carnauba wax and water were numerical materials.

The multiphase model step of carnauba solution was similar to the preliminary of multiphase simulation. Minor differences were made. The first difference, Materials are indicated as carnauba wax and water.

VOF and Mixture model for multiphase flow were tested the prediction to dictate the interactions between the two phases of water and carnauba wax in the system. The result of Mixture model revealed the suitable to prediction the power number with the less time required. In this case mixture model was used for further studied. The multiphase flow model required a primary and secondary phase. This case water was the primary phase (continuous phase) and carnauba wax was secondary phase (dispersed phase).

The others criteria were setup the same as multiphase of preliminary study as previously reviewed.

Table 3.2 Physical property of materials.

Material	Viscosity (kg/m-s)	Density (kg/m^3)
Water (25°C)	0.001003	998.2
Air (25°C)	1.789e-05	1.225
Carnauba solution (85^{0}C)	0.00235	875
Carnauba wax (85^{0}C)	81.296	833
Water (85°C)	0.000334	968

3.4 Grid sensitivity analysis

The five resolutions of meshes were conduct in order to investigate grid sensitive which affect on the prediction of CFD simulation of the transport phenomena inside mixing tank. The refiner mesh was made with the purpose of improving the accuracy of the simulation results.

The adaptive mesh function on FLUENT was utilized to improve mesh to sufficiently capture the changes on velocity gradients region i.e. the area enclose the impeller. FLUENT provided tools to create mesh in various particular applications such as Boundary Adaption, Gradient Adaption, Region Adaption and Volume Adaption. The recommendation of each application described in the Help section of ANSYS FLUENT.

This thesis applied Boundary Adaption function, in order to refine the meshes the area within the boundary of impeller. Boundary adaption was used to create five resolutions of mesh which were: Coarse, Adapt I, Adapt II, Adapt III and Adapt IV. The resolution was increase until the solution had no notable difference and the error from experimental result was decreased. The number of grid resolution was shown in Table 3.3

Table 3.3 The various resolutions of grids creating for grid sensitivity analysis.

Grid number	Case	Number of cell
I	Coarse	86,196
II	Adapt I	140,628
III	Adapt II	368,436
IV	Adapt III	1,289,076
V	Adapt IV	4,990,452

3.5 Validation approach

To validate the prediction of CFD model, preliminary and carnauba solution model were calculated torque generated by impeller at various speeds. Then torque datum was converted in term of Power number (N_p) as shown in Equation 1 while Reynolds number (Re) was calculated

according to Equation 4 as mention in literature review. The plot relationship between Power number (N_p) in Y‑axis and impeller speed (rpm) in X‑axis was generated. Then the plots derived from experiment and simulation was compared.

3.6 The effect on flow behavior

Since, the flow regime inside the tank represents the mixing behavior within the process. The mixing characteristic also influences the product quality. The relevant parameters in which affected the flow regime or velocity profile were selected to study in this thesis, the effects were discussed in the next section.

3.6.1 Effect of rotational velocity

The qualitative contour and vector plot derived from CFD simulation in which presents flow pattern creates by the impeller help elucidate whether the impeller speed is sufficient to mix or whether there are dead zone in the tank. Comparison of impeller speeds of 2000, 2700 and 2900 rpm affected on flow regime will be discussed.

3.6.2 Effect of fluid viscosity

When the material property is changed, the Re number is also changed. Two ranges of Reynolds number are investigated using water and carnauba solution. At the same rotational speed of 2000 rpm, the velocity profile of water and carnauba solution will be compared. Detailed of Re range for two working fluids were given in Table 3.4.

Table 3.4 Viscosity of water and carnauba solution.

Working fluid	Viscosity (kg/m-s)
Water	0.001003
Carnauba solution	0.00235

3.7   Scale up study

As mention in introduction, this thesis is also aim to investigate the effect of different scale up criteria so that we can guide the suitable criteria.

3.7.1   Dimension of large-scale tank

The large-scale tank figure was similar to lab-scale tank. The configuration of the tank was conducted by adjusting the scale of the lab-scale tank from millimeter to centimeter (i.e., scale up by 1000 times). Selecting the Scale on FLUENT, changed the unit of all coordination into centimeter. The 220 cm diameter (T) large-scale tank consisted of a 6-blade impeller with 29 cm diameter (D) was equipped at 44 cm clearance from the tank wall (off-center) and 11.4 cm from the bottom.

This thesis employed the scale up criteria i.e. Reynolds number (Re), Froude number (Fr) and impeller tip speed (V_{tip}) which was individually kept constant. The Reynolds number (Re) and Froude number (Fr) are based on conservation of force ratio. Impeller speed tip (V_{tip}) is based on rate of agitation.

3.7.2   Reynolds number (Re) constant

The desire is to have the same hydrodynamic large scale as small scale. This can be written as an equation:

$$\text{Re} = \frac{\rho N D^2}{\mu} \tag{1}$$

$$\text{Re}_1 = \text{Re}_2$$

$$N_1 D_1^2 = N_2 D_2^2$$

$$N_2 = \frac{D_1^2 N_1}{D_2^2} \tag{1.1}$$

3.7.3   Froude number (Fr) constant

The desire is to have the same vortex formation in large scale as in small scale. This can be written as an equation:

$$Fr = \frac{DN^2}{g} \qquad (2)$$

$$Fr_1 = Fr_2$$

$$\frac{D_1 N_1^2}{g_1} = \frac{D_2 N_2^2}{g_2}$$

$$N_2^2 = \frac{D_1 N_1^2}{D_2} \qquad (2.1)$$

3.7.4   Impeller tip speed (V$_{tip}$) constant

The desire is to have the same the agitation rate of large scale as in small scale. This can be written as an equation:

$$V_{tip} = \pi ND \qquad (3)$$

$$V_{tip1} = V_{tip2}$$

$$N_1 D_1 = N_2 D_2$$

$$N_2 = \frac{D_1 N_1}{D_2} \qquad (3.1)$$

CHAPTER IV

RESULTS AND DISCUSSION

4.1   Grid sensitivity analysis

Change of grid type and resolution will give effect on the accuracy of numerical results and computational time. The reasonable or acceptable grid type and resolution which provide consistent simulation results were determined. This thesis employed the technique of adaptive mesh in order to refine the mesh as mention previously in Chapter 3 research methodology.
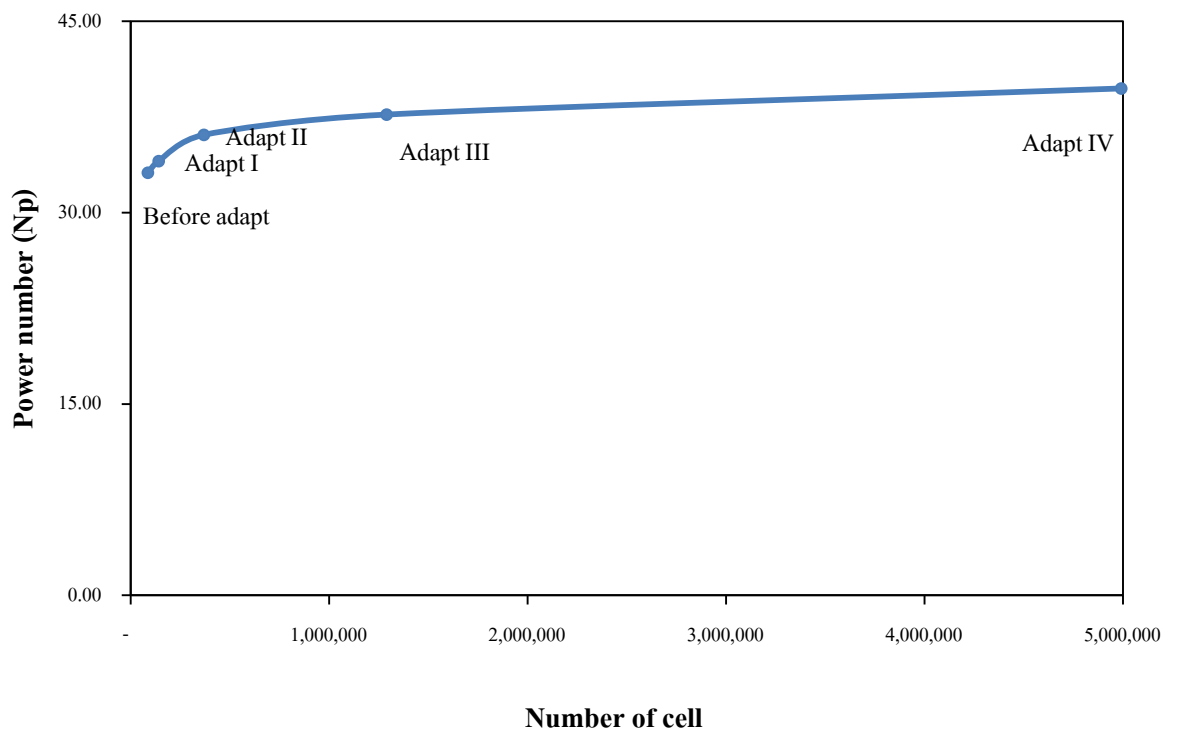

Figure 4.1 The effect of grid resolution on the simulated power number at speed of 2000 rpm.

In this study, the resolution of structured from coarse grid (adapt I: number of cell = 86,196), finer grid resolution in adapt II, III and IV (number of cell = 140,628, 368,436, 1,289,076 and 4,990,452 respectively). This study investigates the effect on power number

prediction. The effect of grid resolution on simulation results of power number and the error range are presented in Figure 4.1 and Table 4.1 respectively.

Figure 4.1 shows that as the mesh was further adapted within the range of 86,196-368,436 cell, the power number prediction was slightly changed. The error range was 4.04 % - 19.99% as shown in Table 4.1.

Table 4.1 The error range of power number prediction at speed of 2000 rpm

2000 rpm	Cell	%Error	Calculation time (hr.)
Before adapt	86,196	19.99	6
Adapt I	140,628	17.80	9
Adapt II	368,436	12.82	13
Adapt III	1,289,076	8.99	18
Adapt IV	4,990,452	4.04	24

The error was decreased after increasing the adaption, however longer computational time is required. This study employed the adapt II, grid resolution of 368,436 cells due to its prediction and computational time was within an acceptable tolerance. Even if increasing the further adaption in order to obtain lower error, much longer calculation time is required. Thus the Adapt II was then applied to all cases of further studies.

4.2   Preliminary study

The preliminary study was carried out with two purposes, the first one was to evaluate the accuracy of validation experimental method. The experiment was set up to measure power using multi-meter. The second one was to compare the influence of viscosity between water and carnauba solution on flow behavior.

4.2.1   Experiment

The experiment was carried out to measure power using multi-meter at various speeds. The data of current (amperes) were collected while carnauba solution was mixing at various

impeller speeds from 2000 to 2900 rpm. The constant potential difference (volts) was also measured.

Speed (rpm)	Current (I, amperes)	Power (P, watts)
2000	0.11	24.40
2100	0.11	24.85
2200	0.11	25.31
2300	0.11	26.11
2400	0.12	26.90
2500	0.12	27.93
2600	0.13	29.30
2700	0.15	33.29
2800	0.16	37.39
2900	0.17	39.67

Table 4.2 Current measurement data at potential difference 228 volts for preliminary study.

Speed (RPM)	Power (Watt)	Power number (N_p)	Reynolds number (Re)
2000	24.40	32.17	27,899
2100	24.85	28.31	29,294
2200	25.31	25.07	30,689
2300	26.11	22.64	32,084
2400	26.90	20.53	33,479
2500	27.93	18.86	34,874
2600	29.30	17.59	36,269
2700	33.29	17.84	37,664
2800	37.39	17.97	39,059
2900	39.67	17.16	40,454

Table 4.3 Calculation result of Power number and Reynolds number from the preliminary study.

As the form of Equation 10, power (watts) can be calculated. The result of power calculation was shown in Table 4.2. This table shows that as increasing impeller speed, the current and power required for rotating impeller was subsequently increased.

From Equation 1 and Equation 4, the Reynolds number (Re) and Power number (N_p) can be calculated. The result of Power number and (N_p) and Reynolds number (Re) was presented in Table 4.3. This table illustrates that since the impeller speed was increased, Reynolds number (Re) was increased whereas N_p was creased. The range of relative standard deviation among the replicate experiments was 0%-2.9% which means the repeatability of power measurement is satisfied.

The data of relationship between N_p and Re were then plotted in a log-log plot as shown in Figure 4.2.
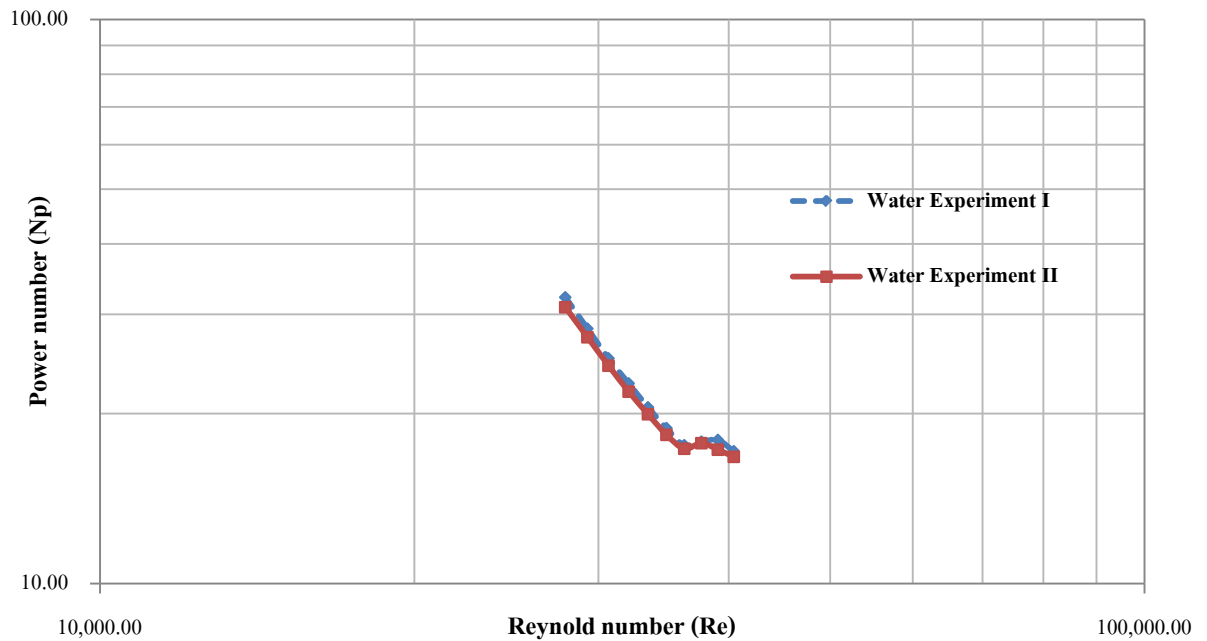
Figure 4.2 Power curve from preliminary study.

The power curve in Figure 4.2, Power number (N_p) is inversely proportional to Reynolds number (Re). It is because solid body rotation depresses the relative velocity between the fluid and the impeller blade [50]. As a result, the flow motion of water can be theoretically described by laminar flow.

4.2.2 Simulation

The simulation was developed based on two models: single phase and multiphase model. The different assumption among two models were, the effect of air was neglected for the single phase model while was accounted in multiphase model. The governing equation of each phase for multiphase model was additionally calculated.

4.2.2.1 Single phase model

Viscous model for laminar flow was applied. The modeling was set up to simulate at various impeller speeds of 2000 rpm, 2500 rpm and 2900 rpm which correspond to the Reynolds

number of 27,899, 34,874 and 40,454 respectively, in order to calculate torque at each impeller speed. The torque is generated by the result of fluid forces impart on impeller surfaces which can be divided into two contributions [51]:

- The pressure contribution is generated by pressure force which applies in a perpendicular position to the surface of impeller.

- The viscous contribution is generated by the shear stresses applied in tangential position.

The torque also can be calculated from the moment vector on rotating axis (z-axis) by summing the product of force vector with the moment arm vector. The FLUENT code provides the capability to automatically calculate torque by this calculation. Consequently, the torque value is converted into Power number as presented in Equation 3 while Reynolds number can be calculated as Equation 4.
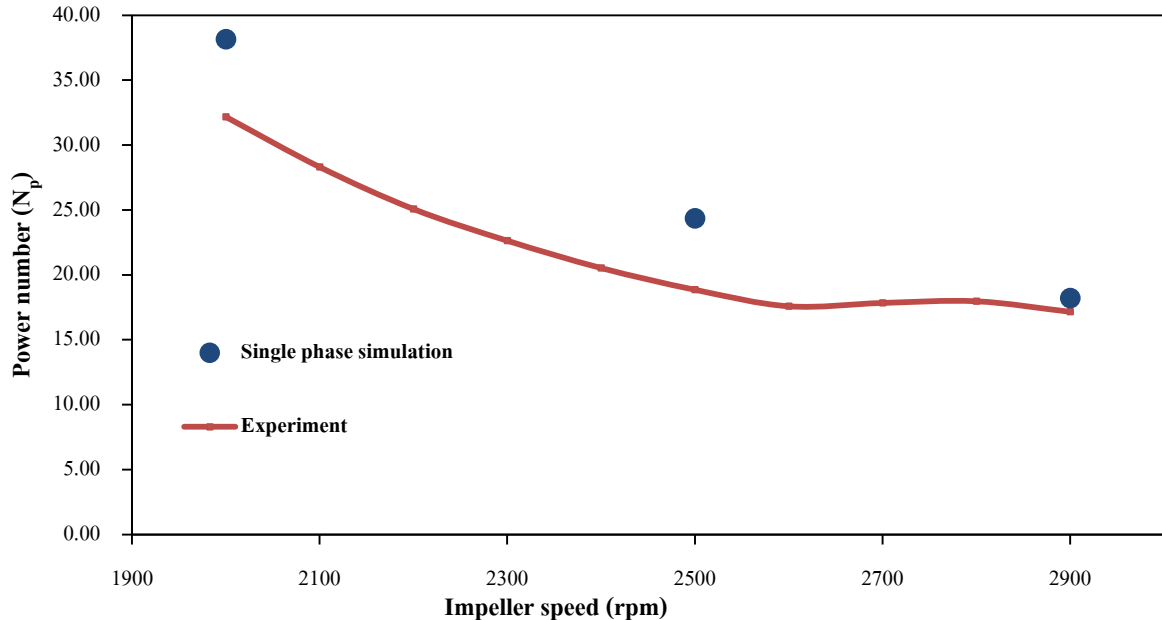
Figure 4.3 Power curve of single phase simulation from preliminary study.

Then the data of relationship between N_P and Re were plotted in a log-log plot as depicted in Figure 4.3. Comparison of experiment and single phase simulation can be made as shown in Figure 4.3.

4.2.2.2 Multiphase model
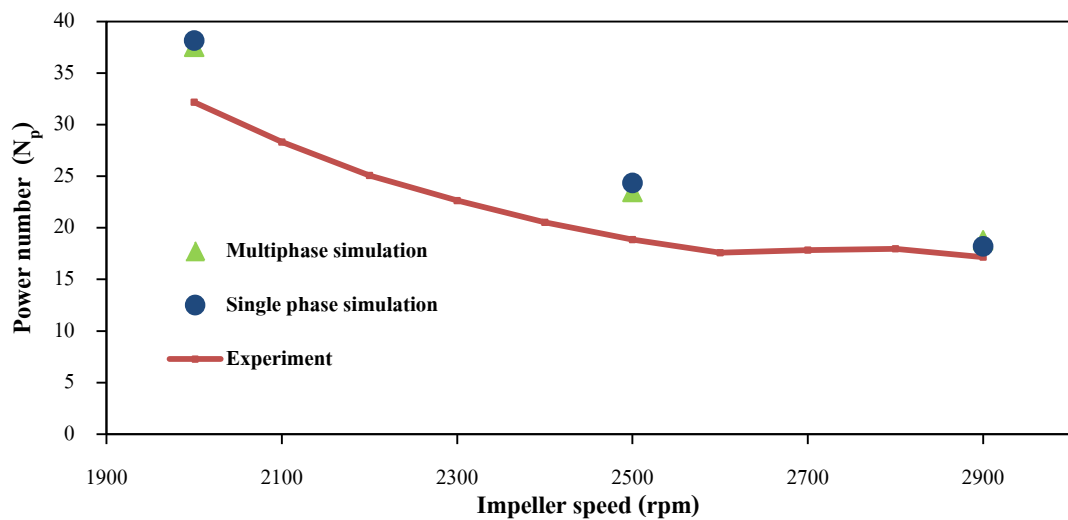
Figure 4.4 Comparison between power curve of single phase and multiphase simulation from preliminary study.

In multiphase system, air was introduced in the top of the tank. The VOF multiphase flow model was employed to investigate the accuracy of prediction. VOF model was enabled in order to solve the momentum equation for each phase.

By the same means of single phase simulation excepting for minor difference in setting up step as mentioned in Chapter 4 research methodology, the multiphase simulation can be developed as illustrated in Figure 4.4. This figure shows that single phase and multiphase simulation for preliminary study give nearly value of Power number in which their error are presented in Table 4.3

Table 4.4 Comparison of percent error between single phase and multiphase simulation

rpm	%Error of single phase simulation	%Error of multiphase simulation
2000	23.51	21.55
2500	32.72	27.96
2900	8.56	12.05

The reason of single phase simulation is not far from multiphase simulation, the interaction of air may not much affect the mixing system. Thus the simplified single phase model based on assumption of air ignored will be reasonable used.

Since in mixing process, power consumption is the parameter influenced heat and mass transfer process, the accurate estimation of power consumption in mixing tank is crucial factor for operation, design and scaling-up the process [52]. As the simulated result of torque prediction which can be convert into power consumption, it proves that validated CFD simulation can be used as the tool of our studies and can be applied to another similar cases.

From these results, we can infer that the preliminary study achieved the first objective. The power measurement to obtain power curve (Power number versus Reynolds number) is efficiency method to validate the simulation result. Then, preliminary study can be applied to carnauba solution study.

4.3 Carnauba solution study

The carnauba solution study has been applied from the preliminary study, however a few modification of the model is properly made.

4.3.1 Experiment

After carnauba solution was prepared, the power was measured using multi-meter. The data of power was collected at speed from 2000 rpm to 2900 rpm and carried out as same procedure as preliminary study.

Speed (rpm)	Current (I, amperes)	Power (P, watts)
2000	0.12	41.42
2100	0.11	35.16
2200	0.11	29.22
2300	0.11	26.52
2400	0.12	24.18
2500	0.12	21.94
2600	0.12	20.16
2700	0.13	19.03
2800	0.13	17.46
2900	0.14	16.18

Table 4.5 Current measurement data at potential difference 228 volts for carnauba solution.

Speed (RPM)	Power (Watt)	Power number (N_p)	Reynolds number (Re)
2000	26.22	39.45	10,438
2100	25.76	33.48	10,960
2200	24.62	27.83	11,482
2300	25.54	25.26	12,004
2400	26.45	23.03	12,526
2500	27.13	20.90	13,047
2600	28.04	19.20	13,569
2700	29.64	18.12	14,091
2800	30.32	16.63	14,613
2900	31.24	15.41	15,135

Table 4.6 Calculation result of Power number and Reynolds number from carnauba solution study.

The experimental data on the impeller speed and power required, as well as the corresponding Reynolds and power number, from the agitation of carnauba solution are shown in Table 4.6. Description can be made that when impeller speed is increasing, it produces the increasing power consumption of mixing.

From Equation 1 and Equation 4, Reynolds number (Re) and Power number (N_p) can be calculated. The results are shown in Figure 4.5. The power curve in Figure 4.5 shows that the flow motion of carnauba solution can be theoretically characterized that the flow exists in laminar region due to the Power decreases with increasing Reynolds number.
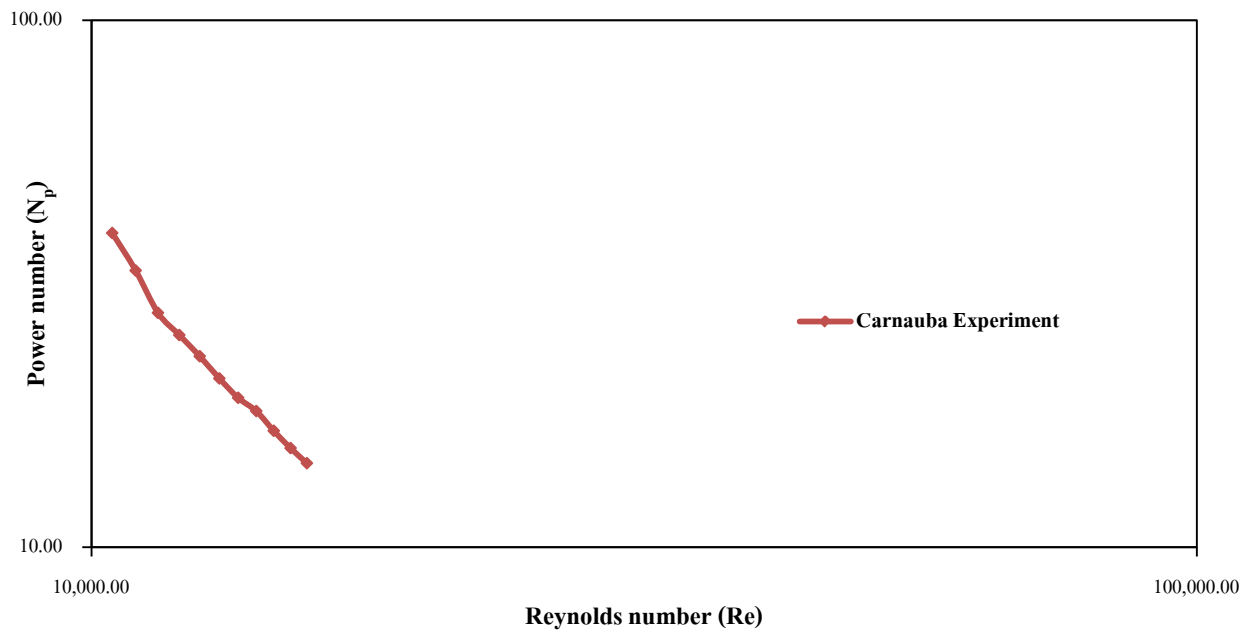
Figure 4.5 Power curve of carnauba solution study obtained from the experiment.

4.3.2   Simulation

4.3.2.1   Single phase model

Figure 4.6 depicts the validation result of single phase model. As figure illustrates, power number represents the effective transmission of energy to the fluid by the rotational of impeller. The relationship was inversely proportional in laminar region.
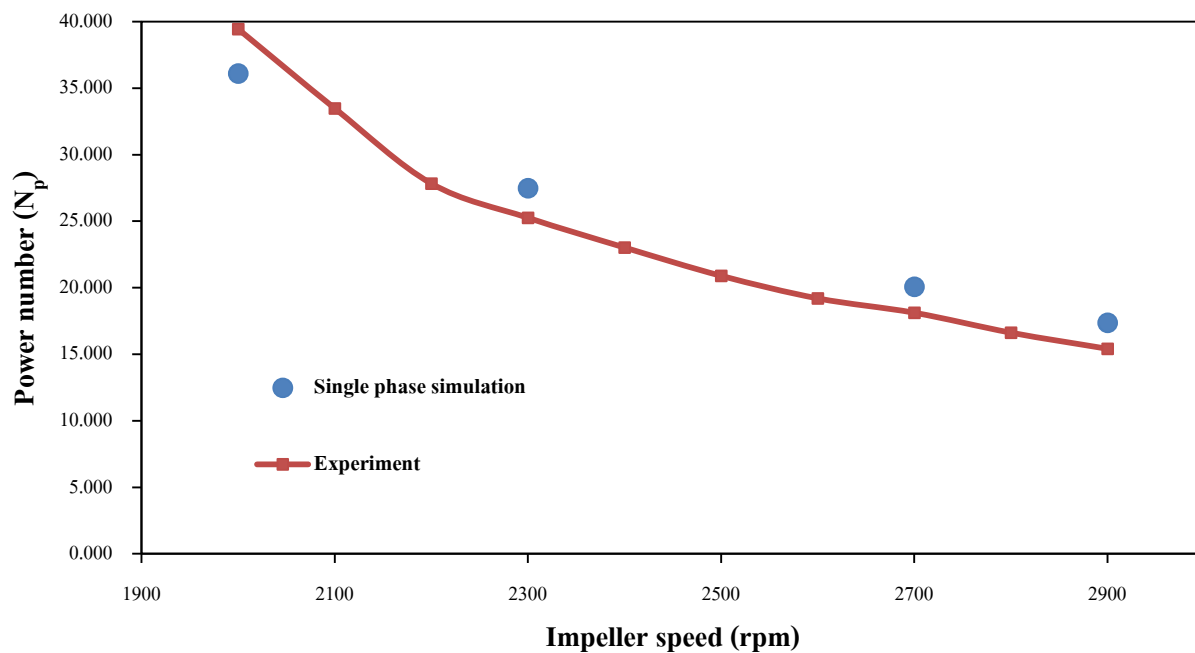
Figure 4.6 Power curve of single phase simulation of carnauba solution study.

4.3.2.2 Multiphase model
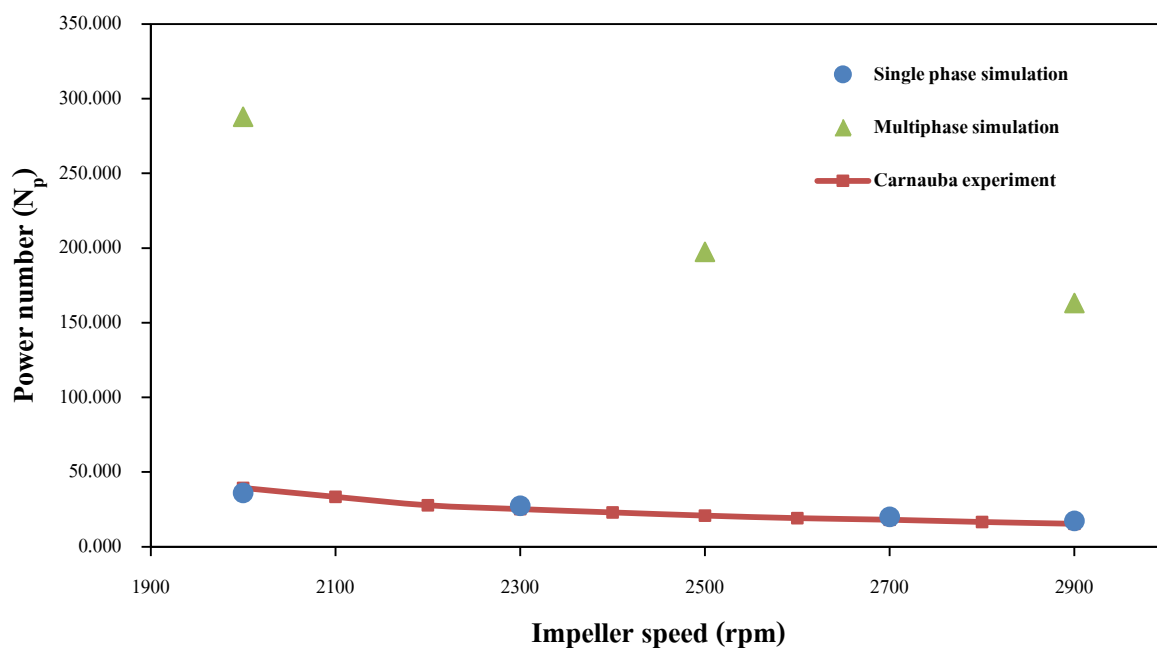
Figure 4.7 Comparison between power curve of single phase and multiphase simulation from carnauba solution study.

After the failure of chosen VOF model as a result of the residual plot was not converged. This may be a result of using the viscosity ratio of fluid is more than $1x10^{3}$. In this case VOF model is found convergence difficulties as proposed by FLUENT [34]. The mixture model is successively employed, it solves the mixture momentum equation for mass-averaged mixture velocity and solves a volume fraction transport equation for secondary phase. The mixture found convergence.

Figure 4.7 depicts the deviation of single phase and multiphase simulation from that experiment of power number prediction. As illustration, the result of single phase model gives obviously satisfaction to the experiment. Multiphase model seem to make large number of error from experiment. One cause that the multiphase model given the results in more error was simplifying the experimental material (81 % water, 5 % carnauba wax, 9 % ammonia and 5 % oleic acid). The most quantity of material using for multiphase model (carnauba wax and water) may lead deviated from actual properties of carnauba solution comparing to single phase model. Thus more accuracy of single phase has been resorted to the further studies. Single phase simulation can give sufficiently valuable information which describes both the qualitative and quantitative behavior of mixing. In this present work, single phase simulation result was then post-processed in order to study these follows topics.

4.4   Flow behavior

Since flow pattern is very important to determine the mixing performance inside the tank, in this section, we study the qualitative analysis of velocity flow field of agitation to examine the structure of the flow for laminar mixing.
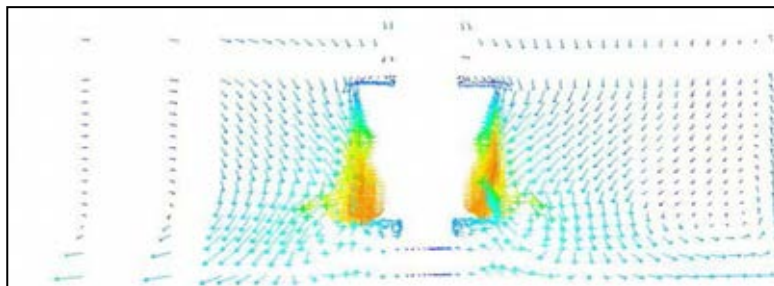
The results of simulation are illustrated by Figure 4.8 a), b) and c). Figure 4.8 a) presents the velocity contour at impeller speed of 2000 rpm.

49

a)

Upper loop

Lower loop
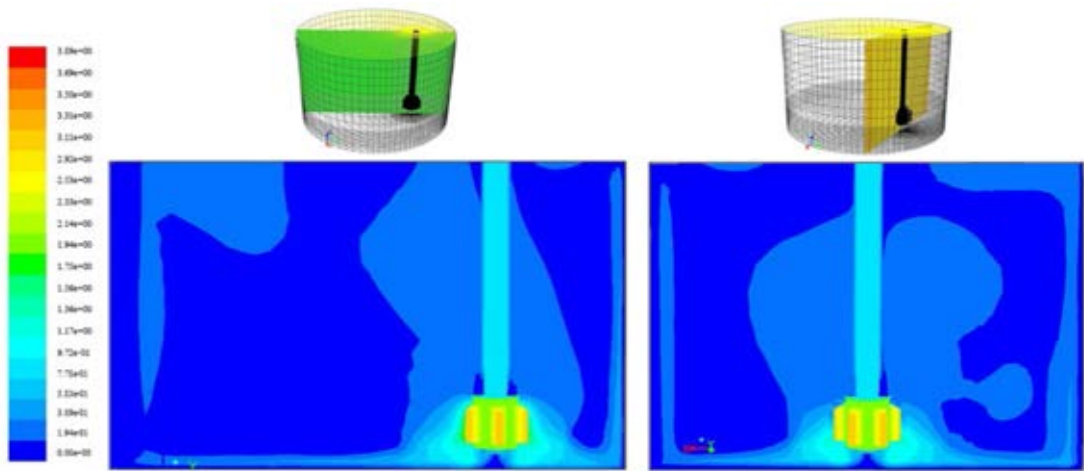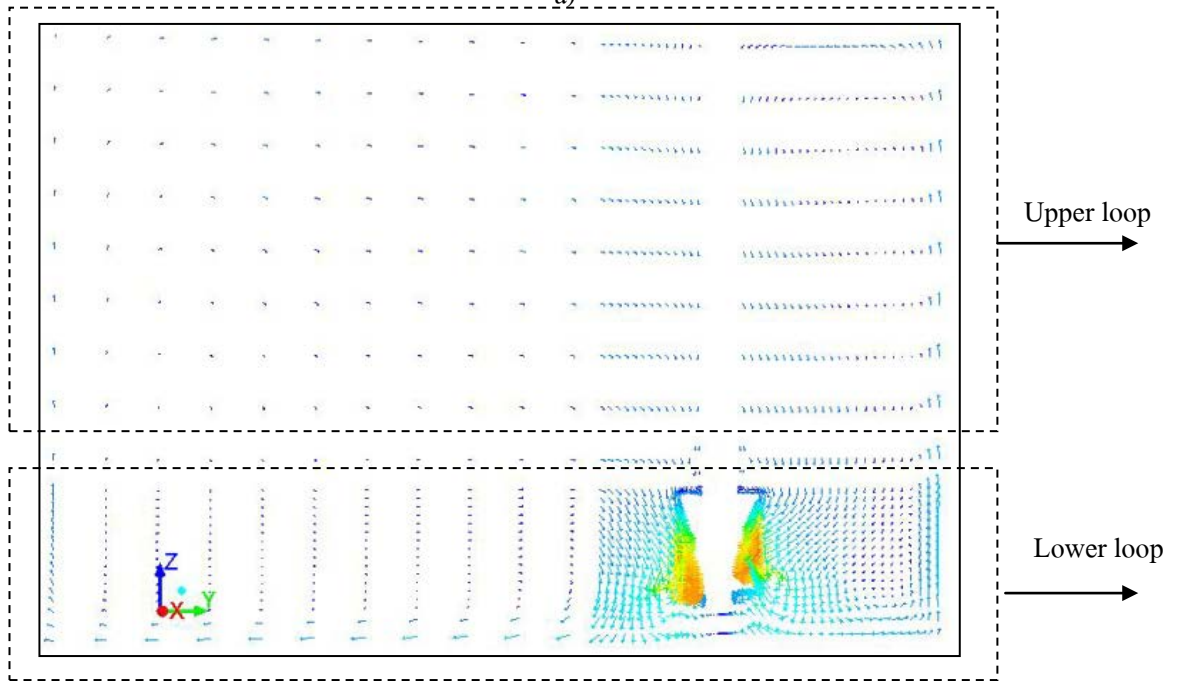
b)

c)

Figure 4.8 Flow patterns at impeller speed of 2000 rpm:

a) Contours of velocity on the two cross-sectional planes,

b) Profile of velocity vector through a cross-sectional plane,

c) Closed-up profile of the velocity vector around the impeller.

Figure 4.8 a) displays that the region around the impeller persist higher velocity than the other region which is far away. The flow field in Figure 4.8 b) demonstrates the characteristic pattern of the 6-blade impeller, equipped off-center. The velocity of fluid flow discharges axially from the blades. The circulation zones are split into two loops i.e. upper and lower of circulation, the fluid is mixed axially to the top and bottom of the tank. The first loop of circulation is zone near the impeller and the other is above the impeller. As can be seen, the second loop of fluid flow of the both sides of the tank seems to be stagnant elsewhere, however the side which the impeller is near tank wall exhibits the stronger velocity than the other side. This upper loop may become the dead zone which the fluid motion has low velocity, it may cause the velocity to transfer fluid is insufficiently for mixing throughout the tank.
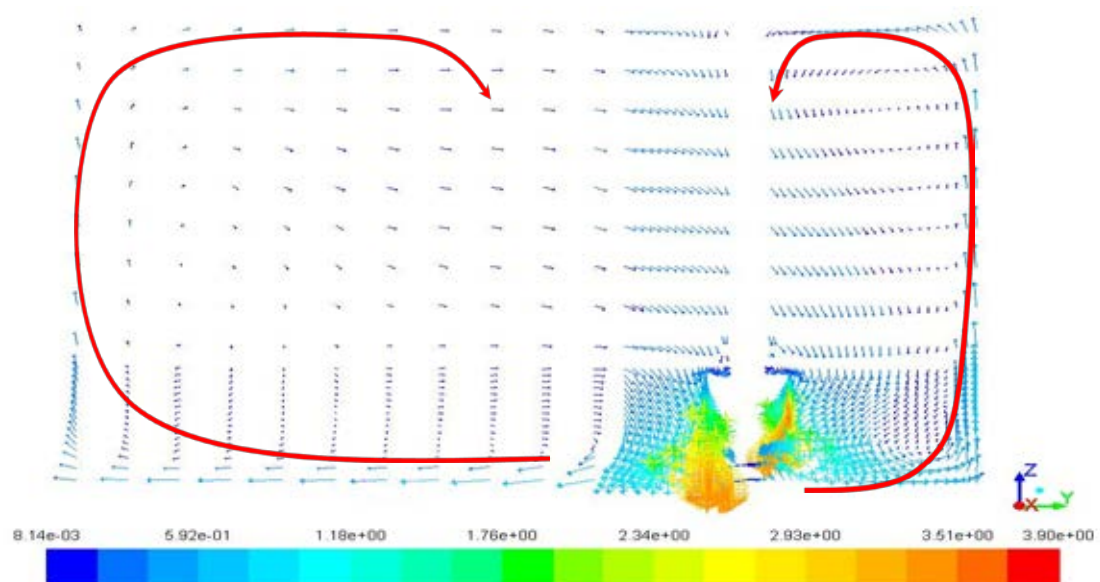
Figure 4.9 Velocity vector represent for overall flow pattern

From the flow pattern in Figure 4.9, its agitating direction determines to be axial mixing. Fluid is pushed up and down along the impeller shaft. Such flow pattern would impose essentially bulk motion mixing.

As previously mentioned in Chapter 2 theory section, the continuity and momentum equation (Equation 7 and 9 respectively) were applied to solve laminar flow in the mixing tank in this study. The steady state momentum can be arraged as Equation 18

$$\underbrace{\nabla \cdot (\rho V V)}_{} = -\nabla p - \underbrace{[\nabla \cdot \tau]}_{} + \rho g \qquad (11)$$

Convection term   Diffusion term

The momentum is can be transfer through fluid the bulk fluid motion which is **convective momentum transport (convecion term)** and also transfer by viscous action which is **molecular momentume transport (diffusion term)** [53].

4.5   Effect of rotational velocity

Since the flow is in laminar region the nonexistence of turbulent diffusion limit the transport across streamlines to relatively slow process of molecular diffusion [53]. In highly viscous fluid, the rate of molecular diffusion is extremely slow, convective momentum is the important part in this section.

Flow pattern of three velocities in Figure 4.10 a, b and c shows that the high velocities are produced in the region close to the impeller. The velocity within the region near impeller and away from that creates large deviation as displayed in different colors. The region away from the impeller motion, decomposed velocities and nearly stagnant fluid are presented at all rotational velocities.
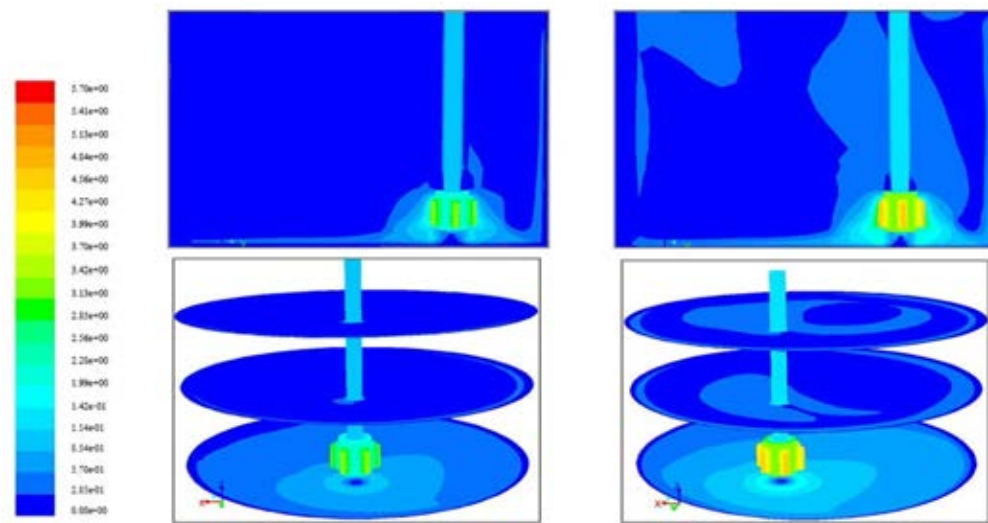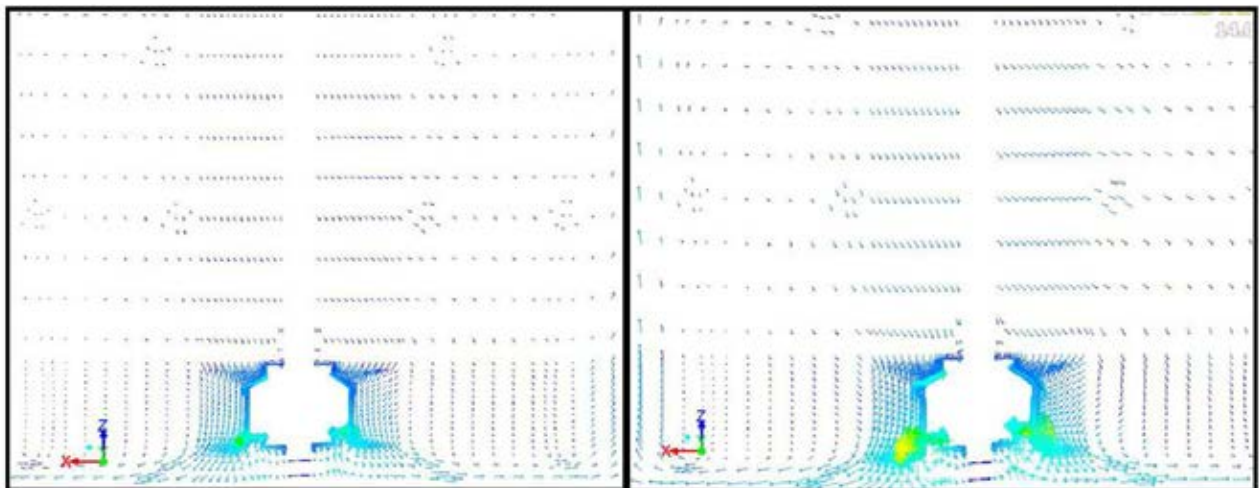
a)   b)

Figure 4.10 Contour of velocity magnitude (m/s)

at speed of a) 2000 rpm, b) 2900 rpm

a)   b)

Figure 4.11 Profile of velocity vector

a) 2000rpm   b) 2900 rpm

At higher impeller speed, the stronger circulations created. As can be seen in Figure 4.11 a) and b), the higher order of magnitude of velocity vector appear in higher impeller speed. The simulated model predicts weak circulations pattern presented by low velocity region which could not affects every part of tank and there may cause insufficient mixing performance.

Increasing rotational velocity affects the flow hydrodynamics and mixing. The higher rotational velocity leads the higher fluid transfer by bulk fluid motion which helps increasing better mixing performance.

4.6   Effect of viscosity

The pattern of fluid flows in mixing tank depends on many factors, e.g. type of impeller, and the characteristic of fluid, especially its viscosity. This section investigates the influence of kinetic viscosity which is a parameter in the term of diffusion term.

In this study, the flow pattern of two fluid i.e. water and carnauba solution possess different Reynolds due to different viscosity is illustrated.

Figure 4.11 a) and b) shows the flow behavior of water and carnauba solution respectively. The considerably difference of flow behavior between two fluids is within the region far away from impeller. As this figure exhibits, in water mixing the velocity contributes throughout the tank better than carnauba mixing. The low velocity (blue shade) in carnauba solution is more apparent and may contribute to poor mixing performance.
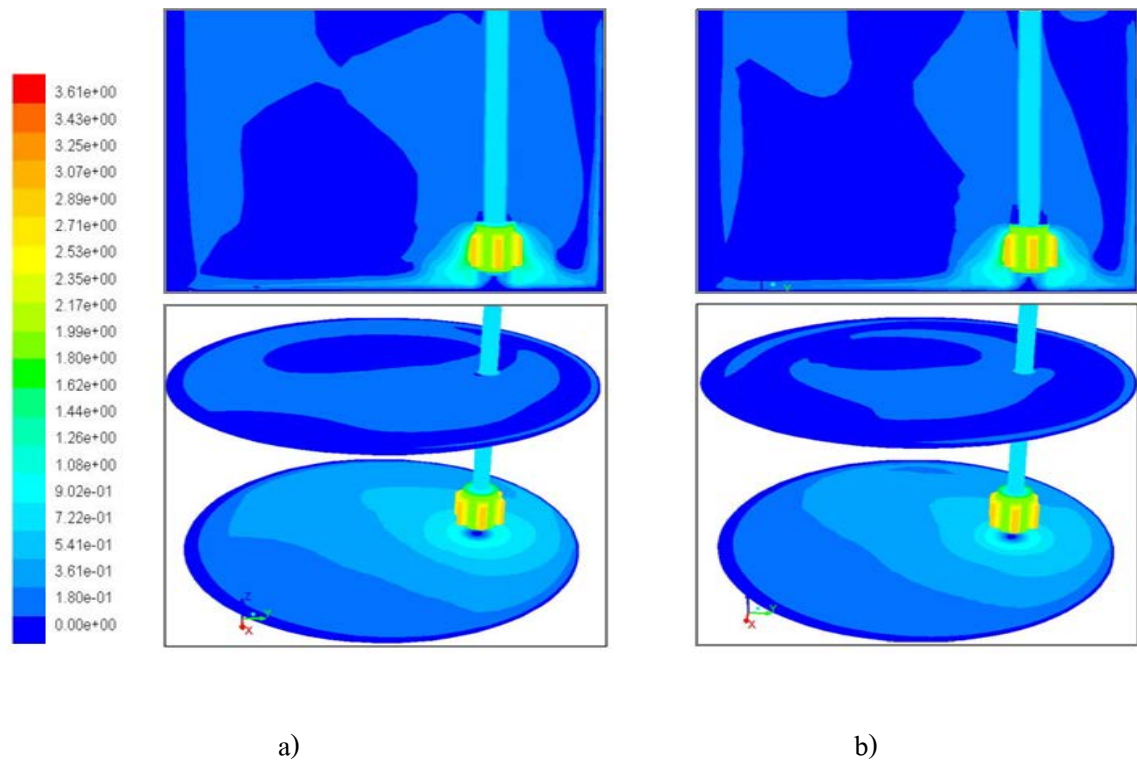
Figure 4.12 Magnitude velocity contours (m/s) at 2000 rpm.

a) cross section plane of water b) cross section plane of carnauba solution.

4.7 Effect of shear stress

Mixing two immiscible liquids produce the production of a disperse phase distributed in other phase as the form of small droplets [54]. Drop size distribution in an agitated dispersion is a result of the dynamic equilibrium which consists of the breaking and coalescing drops, increasing the drop breakage rate or decreasing the drop coalescence rate produces smaller drop sizes. In dynamic flow system, the maximum drop size can be determined by the external deformation forces and restoration forces:

- The external deformation force is the result of turbulent fluctuation and viscous stress due to velocity gradients of surrounding field.

- The restoring force is the result of the interfacial tension and/or the internal viscous stress.

Regarding to Newton's law of viscosity, viscous (shear) stress (τ) this "Momentum flux" example in x-y direction can be expressed as follows:

$$\tau_{xy} = -\mu \frac{dv_x}{dv_y} \tag{12}$$

The Newton's law of viscosity equation or molecular transport of momentum, represents the relation between shear force per unit area and the negative velocity gradients. It describes transfer of momentum component in each direction (for example in equation 5, the x-momentum transmits in y-direction) with velocity gradient as the driving force. The fluid transport happens by intermolecular forces among their surround. Consequently, when shear stress increases the force in which dissipates to breakage of molecules is also higher. The result of shear stress at the impeller speed of 2000 rpm and 2900 rpm shows in Figure 4.13 which is observation in the z-axis between the impeller and tank wall (red line) presented in Figure 4.12. The shear rate is decreased toward from the impeller blades because of moderated velocity. The shear stress found maximum at the tank wall as a result of wall shear stress. This result agrees with Deplano et.al. [55] investigated the wall shear stress analysis.

The higher impeller speed of 2900 rpm generates higher magnitude of shear rate than 2000 rpm. This simulated result may indicate that the higher the mixing performance due to the higher external deforming force (only viscous stress because turbulent fluctuation is absence in our study), the larger the speed of impeller.
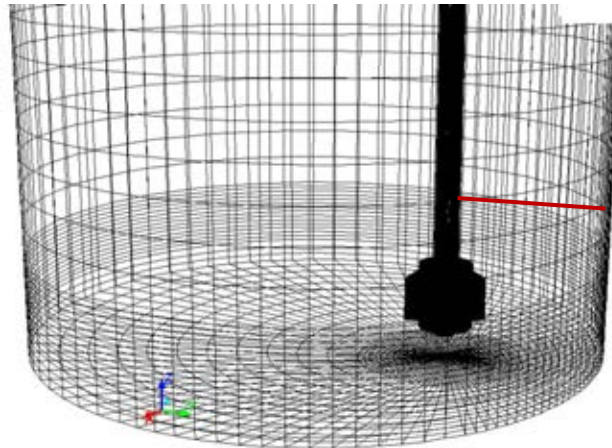
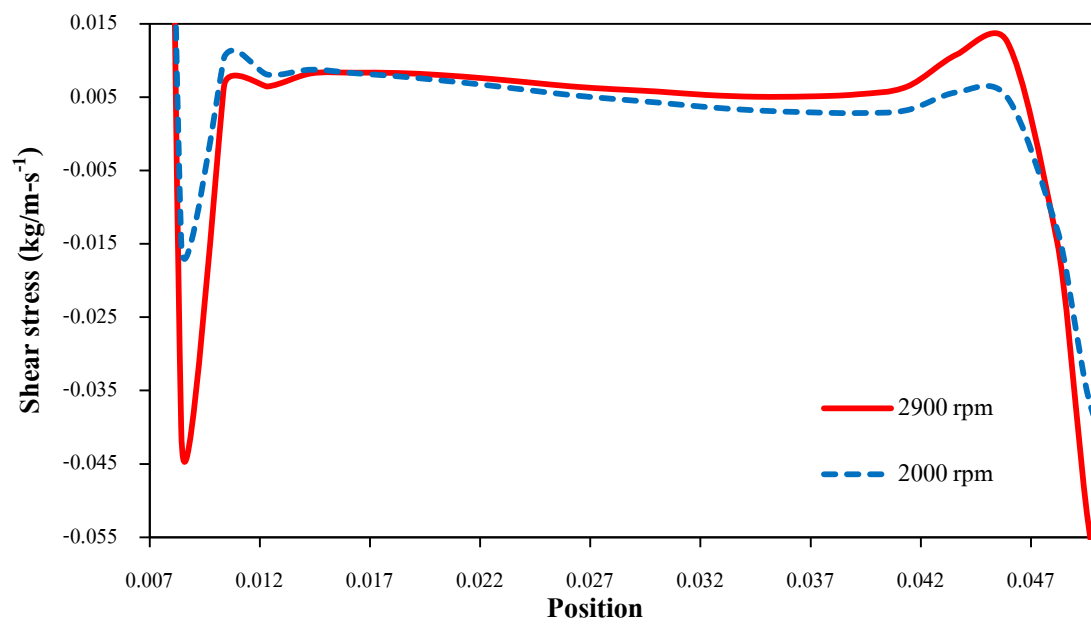**Figure 4.13** Position of shear stress considerations.

Figure 4.14 Shear stress of 6-blade impeller as a function of position.

4.8   Effect of scale-up criteria

Once the flow regime and its influence have been studied, the validated model of single phase simulation is then employed to large-scale tank. As previously mentioned in Chapter 2, the scale up criteria based on similarities can be expressed in term of the geometrical similarity,

kinematic similarity and dynamic similarity. In this research followed the geometric similarity and kinematic principle. Geometric similarity is really not needed but serves as a starting point for scale up [56]. The same configuration of the lab-scale and large-scale tank was conducted so that the fluid motion of the small and large sizes was assumed to be similar. A result, geometric similarity provides kinematics similarity [57]. The kinematic similarity refers to the motion and the same ratio of velocities for the corresponding positions in the mixing tank.

The different scale-up criteria i.e. Reynolds number (Re) constant, Froude number (Fr) constant and Impeller tip speed (V_{imp}) constant are summarized. Results of normalized velocity with normalized position of each scale-up criteria represented kinematic comparison. The simulated result of velocity profile in Figure 4.15 shows the normalized velocity derived from various scale-up criteria. The scale up criteria of Fr constant, Re constant and V_{tip} constant is still not accomplished.
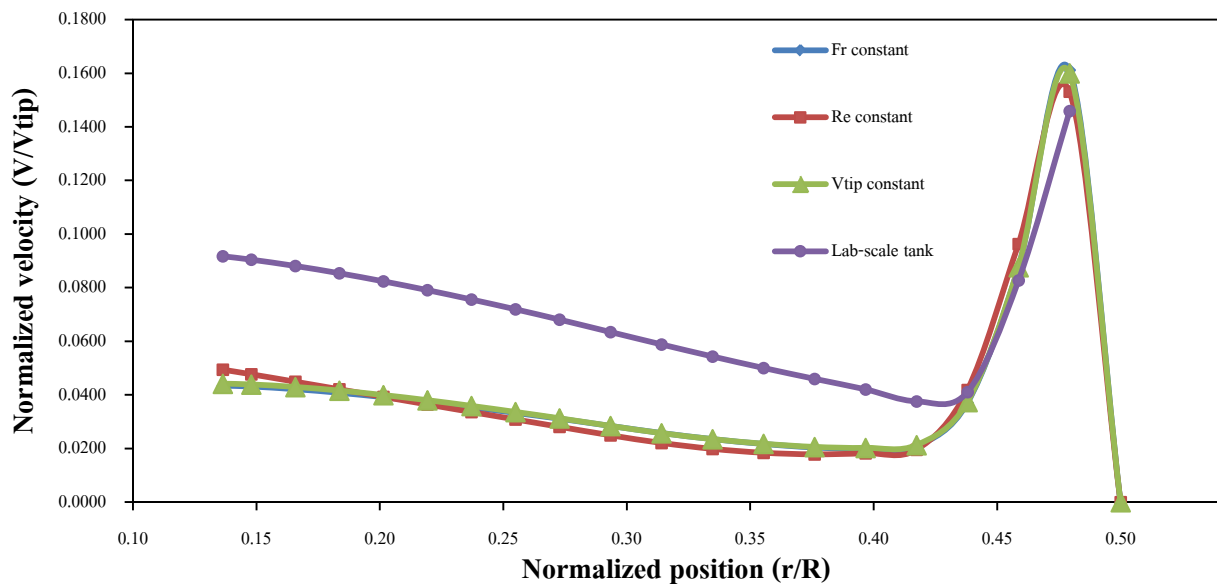
Figure 4.15 Velocity profile over the axial position derive from various scalu-up criteria.

CHAPTER V

CONCLUSIONS AND RECOMMENDATIONS

Conclusions

In this thesis, Computational Fluid Dynamics simulations have been developed to study the transport phenomena inside the mixing tank of carnauba solution. The flow regime of 6-blade impeller which equipped off-center has been investigated. Then, the scale-up criteria is summarized. The conclusions relating to research objectives are followings:

1.2.1   To develop a suitable CFD model to study fluid dynamic of carnauba solution inside the mixing tank.

- CFD modeling was successfully developed and applied to study the flow behavior inside the mixing tank based on assumption of laminar and steady state flow.

1.2.2   To study the phenomena of fluid mixing using the validated CFD model.

- 6-blade impeller equipped off-center used in carnauba solution mixing the tank was introduced and the resulting flow pattern was investigated using CFD simulation.

- Increasing rotational velocity, the mixing performance was increased.

- Decreasing viscosity, the mixing performance was increased.

- Increasing shear stress (increasing rotational velocity), the particle size would be decreased.

1.2.3   To summarize and guide the scale-up criteria for carnauba solution tank.

- The scale-up criteria of Fr constant, Re constant, Vtip constant are not accomplished the kinematic similarity.

Recommendations

- This study gives better understanding of the flows within the mixing tank with 6-blade impeller which mounted off-center. However it should be noted that this study is subject to modeling assumption of laminar and steady state flow. There are still rooms for improvement the model to be more realistic. Lessen assumptions should be required.

- Optimum condition in lab-scale tank should be ensured before applying to CFD modeling.

- Other criteria could be further considered such as Webber number constant and Power energy constant which based on the emulsion size of the emulsion was the same [58]. Moreover, more than one criterion should be kept constant such as Reynolds number and Froude number (Fr).

REFERENCES

[1]   Salakpetch, S. Hawaii tropical fruit growers. Tenth annual international tropical fruit. 2000. Hilo, Hawii.

[2]   Mingzhong Li, G.W., Derek Wilkinson, Kevin J. Roberts. Scale up study of retreat curve impeller stirred tank using LDA measurement and CFD simulation. Chemical Engineering Journal, 2005. 108: p. 81-90.

[3]   Morton, J.F. In: Fruits of warm climates, 1987: Miami, Fl. p. 262–265.

[4]   Sakulwong, K. Effect of Shellac Coating Formulations Containing Shellac Wax or Carnauba Wax Combined with Composite Plastic Bags on the Shelf Life of Rambutan cv. Rongrien. Agricultural Sci. J. , 2011. 42 : 1 (Suppl.): p. 275-278.

[5]   Shaw, R.D.H.P.E. Gas Permeability of Fruit Coating Waxes. J. AMER. SoC. HORT. SCI, 1992. 117: p. 105-109.

[6]   Tibiro, C. Optimization of edible coating composition to retard strawberry fruit senescence. Postharvest Biology and Technology, 2007. 44: p. 63-70.

[7]   B., M., Perez-Gago, and J.M. Krochta. Drying Temperature Effect on Water Vapor Permeability and Mechanical Properties of Whey Protein–Lipid Emulsion Films J. Agric. Food Chem, 2000. 48(7): p. 2687–2692.

[8]   Nagata, S. Mixing: Principle and applications, 1975. 444-447.

[9]   Process Associates of America, D.N., 2004, Online.

[10]   Marina Campolo, A.P., Alfredo Soldati, Fluid Dynamic Efficiency and scale up of a retreated blade impeller CSTR. Ind. Eng. Chem, 2002. 41: p. 164-172.

[11]   Lane, G.L. and P.T.L. Koh, CFD simulation of Rushton Turbine in a baffled Tank, in Inter Conf on CFD in Mineral&Metal Processing and Power Generation. CSIRO, 1997: Victoria 3169, Australia.

[12]   Esfahany, M.H.V.M.N. CFD analysis of turbulence in a baffled stirred tank, a three-compartment model. Chemical Engineering Science, 2009. 64: p. 351-362.

[13]   R.Zadghaffari, J.S.M., J. Revstedt, A study on liquid-liquid mixing in a stirred tank with a 6 blade rushton turbine. Iranian Journal of chemical engineering, 2008. 5(4): p. 12-19.

[14]   Rodi, W. <u>Turbulence models and their applications in hydraulics - a state of art review.</u> International Association on Hydraulic Research, 1980.

[15]   Markatos and N.C., <u>The mathematic modeling of turbulent flows.</u> Applied Mathematical Modelling, 1986. 10: p. 190-220.

[16]   Koh, P.T.L. and F.Xantidis, <u>CFD Modelling in the scale-up of a stirred reactor for the production of resin beads.</u> CFD in the mineral and process industries, 1999: CSIRO, Melbourne, Australia.

[17]   Alexpoulos, A.H., D. Maggioris, and C. Kiparissides. <u>CFD analysis of turbulence non-homogeneity in mixing vessels : A two-compartment model.</u> Chemical Engineering Science, 2002. 57: p. 1735-1752.

[18]   H.S. Pordal, C.J.M. <u>Design, Analysis and scale-up of Mixing Processes,</u> SES-Process Technology Group.

[19]   Nirotanan, N. and P. Pakaprasit, <u>Fruit coating production process developement of shellac and carnauba wax.</u> 2012.

[20]   Kittiwit Sakulwon, A.B., Seeroong Preechanont, Sorada Kanokpanont. <u>Effect of shellac coating formulation containing shellac wax or carnuaba wax combined with composite plasic bag on the shelf life of rambutan cv. Rongrien.</u> Agricultural Sci. J., 2011. 42:1: p. 275-278.

[21]   Oldshue, J.Y. <u>Fluid Mixing Technology</u>. McGraw-Hill, 1983: p. 43.

[22]   Maingonnat JF., D.J., Lefebvre J., Delaplace G. <u>Power consumption of a double ribbon impeller with Newtonian and shear thinning fluids and during the gelation of an iota-carrageenan solution.</u> J Food Eng, 2008. 87(1): p. 82-90.

[23]   Bouvier L., M.A., Line A., Faqtah N., Delaplace G. <u>Damage in agitated vessels of large visco-elastic particles dispersed in a highly viscous fluid.</u> J Food Sci, 2010. 76(5): p. E384-E391.

[24]   Migliori M., C.S. <u>Modelling of dough formation process and structure evolution during farinograph test.</u> Int J Food Sci Technol, 2012. 48(1): p. 121-127.

[25]   Franco JM., D.M., Valencia C., Sanchez MC, Gallegos C., <u>Mixing rheometry for studying the manufacture of lubricatin greases.</u> Chemical Engineering Science, 2005. 60(8-9): p. 2409-2418.

[26]   Dusting J, S.J., Hourigan K. A Fluid dynamic approach to bioreactor design for cell and tissure culture. Biotechnology Bio eng., 2006. 94(6): p. 1196-1208.

[27]   Lin Y., T.J., Pullulan fermentation using a prototype rotational reciprocating plate impeller. Bioprocess Biosys Eng.

[28]   Alvarez MM., A.P., Muzzio FJ., Laminar mixing in eccentric stirred tank system. Canadian Journal of Chemical Engineering, 2002. 80: p. 546-557.

[29]   Holland, F.A. Scale-up in chemical engineering. Chemical and Process Engineerings, 1964. 45(121-4).

[30]   H.S. Pordal, C.J.M., Design, Analysis and Scale-up of mixing process. SES-Porcess Technology Group.

[31]   Murthy Shekhar S., J.S., CFD study of power and mixing time for paddle mixing in unbaffled vessels. Trnas IChemE, 2002. 80(Part A): p. 482-498.

[32]   Eva Stahl Wernersson, C.T. Scale-up of Rushton turbine-agitated tanks. Chemical Engineering Science, 1999. 54: p. 4245-4256.

[33]   Asghar Alizadeh Dakhel, M.R., CFD simulation of homogenization in large-scale crude oil storage tanks. Petroleum Science and Engineering, 2004. 43: p. 151-161.

[34]   ANSYS, I. Theory guide. ANSYS FLUENT 12, 2009.

[35]   Ansys, I. Ansys fluent 12. Theory guide, 2009.

[36]   Placek. Turbulent flow in stirred tanks-Part II. A two-scale model of turbulence A.I.Ch.E Journal, 1986. 32: p. 1771-1786.

[37]   Wood, P.E., K.S.M. Prediction of the three-dimensional turbulent flow in stirred tanks. A.I.Ch.E Journal, 1991. 37(3): p. 448-460.

[38]   Harris, C.K., and Roekaerts, D., Rosendal, F.J.J., Buitendijk, F.G.J., Daskopoulos P., Vreenegoor, A.J.N.&Wang, H. Computational fluid dynamic for chemical reactor engineering. Chemical Engineering Science, 1996. 51(10): p. 1569-1594.

[39]   Montante, G., Lee, K.C., Brucato,A., Numerical simulations of the dependency of flow pattern on impeller clearance in stirred vessel. Chemical Engineering Science, 2001. 56: p. 3751-3770.

[40]   Engh, T.A., D.L.J.S.T., Flow induced by an impeller in an unbaffled tank-I. Numerical modeling. Chemical Engineering Science, 1994b. 49(20): p. 3511-3518.

[41]   Deglon, D.A. and C.J. Meyer. CFD modeling of stirred tanks : Numerical considerations. Mineral Engineering, 2006. 19: p. 1059-1068.

[42]   ANSYS, I. Multiphase flows. Customer Training Material, 2010.

[43]   D. Shapple, S.M.K., A. Wall and A. Afacan. The effect of impeller and tank geometry on power number for a pitch blade turbine. Trans IChemE, 2002. 80: p. 364-371.

[44]   Jean Philippe Torre, D.F.F., Thierry Lasuye, Catherine Xuereb. Single and multiphase CFD approches for modelling partially baffle stirred vessle: Comparison of experiment data with numerical prediction. Chemical Engineering Science, 2007. 62: p. 6246-6262.

[45]   A.W. Nienow, N.H., M.F. Edwards. Mixing in the Process Industries. 3 ed. 1997.

[46]   Nirotanan, N. and P. Pakaprasit. CFD modelling in the scale-up of a mixing tank for the production of shellac-wax fruits coating solution, 2012.

[47]   AlChE. Mixing Equipment (Impeller type). AlChE Equipment Testing Procedure, ed. Thrid.

[48]   Hannah Duscha, M.H., Countney Sparrell. Computational Fluid Dynamics Analysis of Two Phase Flow in Pack Bed Reactor. (Worcester Polytechnic Institute), 2012.

[49]   A. Ghobadian, S.A.V. A General Purpose Implicit Coupled Algorithm for the Solution of Eulerian Multiphase Transport Equation, In International Conference on Multiphase Flow 2007: Leipzig, Germany.

[50]   Hugo A. Jakoben, M.M., Arne Grislingas. Stirred tank reactor. Lecture notes in subject SIK 2053 Reactor Technology.

[51]   Chiu, Y.-T.M. Computational Fluid Dynamic simulations of hydraulic energy absorber. Mechanical Engineerign1999.

[52]   Mahsa Taghavi, R.Z., Jafarsadegh Moghaddas, Yousef Moghaddas. Experimental and CFD investigation of power consumption in a dual Rushton turbine stirred tank. Chemical Engineering Science, 2011. 89: p. 280-290.

[53]   R.Byron Bird, W.E.S., Edwin N. Lightfoot. Transport Phenomena, John Wiley&Sons, Inc. ed. 2. 1924.

[54]   Sechremeli D., S.A., Stamatoudis M. Comparison of mean drop sizes and drop size distributions in agitated liquid-liquid dispersion produced by disk and open type impellers. Chemical Engineering Journal, 2006. 117: p. 117-122.

[55]   V. Deplano, M.S. <u>Experimental and numerical study of pulsatile flows through stenosis: Wall shear stress analysis.</u> Journal of Biomechanics, 1999. 32: p. 1081-1090.

[56]   Gary Tatterson, G.B. <u>Process Scaleup and Design.</u> 2002.

[57]   Uhl, V.W., Von Essen. <u>Scale-up of equipment for agitating liquid.</u> Mixing Theory and Practice, 1986. 3: p. 199-264.

[58]   Jinli Zhang, S.X., Wei Li, <u>High shear mixers: A review of typical applications and studies on power draw,flow pattern, energy dissipation and transfer properties</u>. Chemical Engineering and Processing: Process Intensification, 2012. 57-58: p. 25-41.

APPENDICES

APPENDIX A

ANSYS FLUENT SOLUTION METHOD OF PRELIMINARY STUDY

Variables input for FLUENT Single phase (pure water)

Step 1: Problem setup

1. The FLUENT program was opened in three dimensions according to the geometry and mesh generation. Parallel option was selected where number of processes were depended on the number of CPU possess by individual computer.
    Click OK.
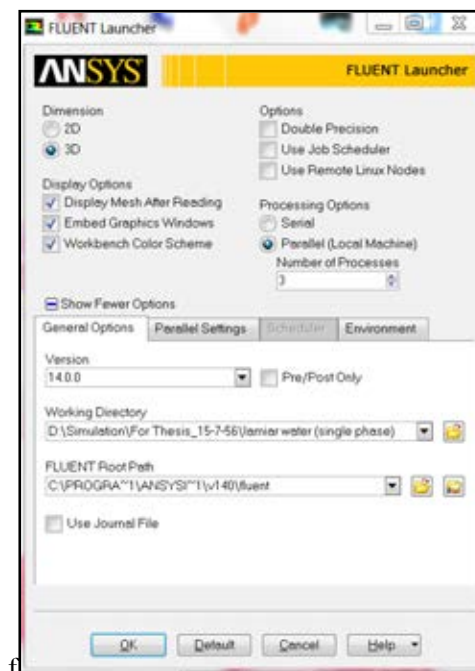
2. The exported mesh file from GAMBIT was imported into FLUENT program.

    File > Read > Mesh
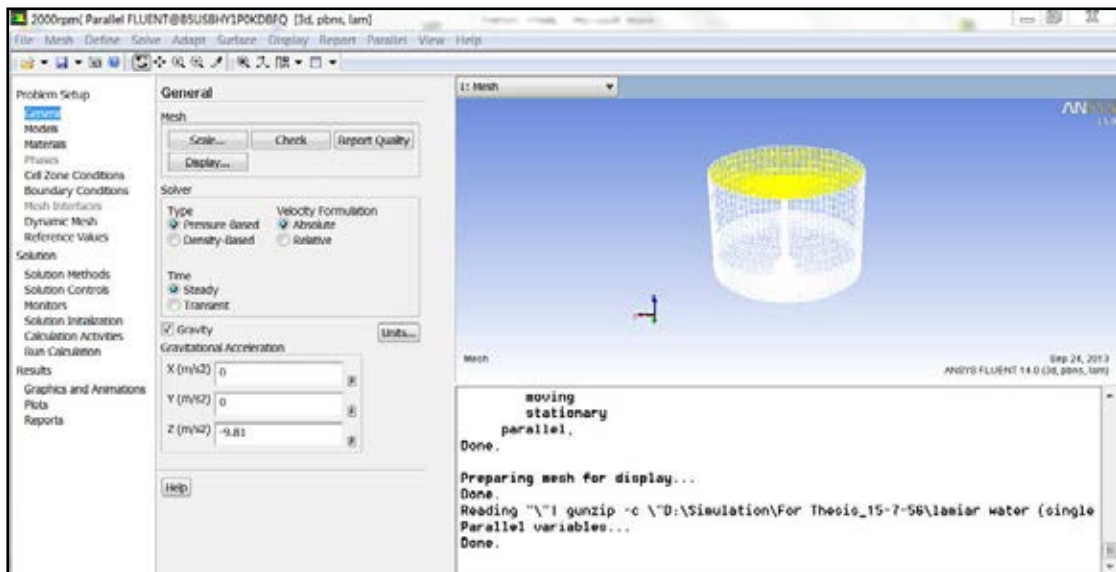
3. Check the mesh.

   Mesh > Check

4. When lunch to FLUENT software, general information was input, pressure-based, steady state with absolute velocity formulation and gravity of 9.81 m/s^2 in negative z direction (the direction of impeller shaft rotated inversely with the **gravitational acceleration**).
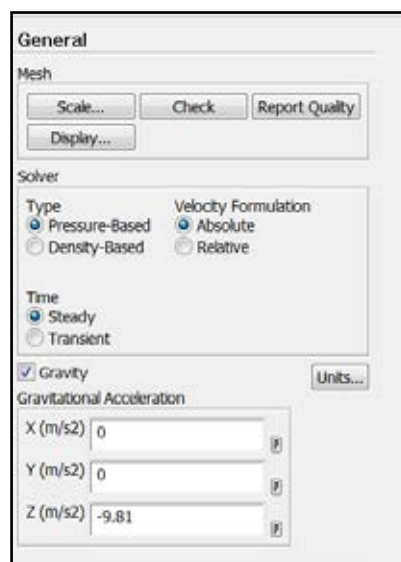
5. Chang the unit of angular velocity as rpm and length as mm

Units > Quantities
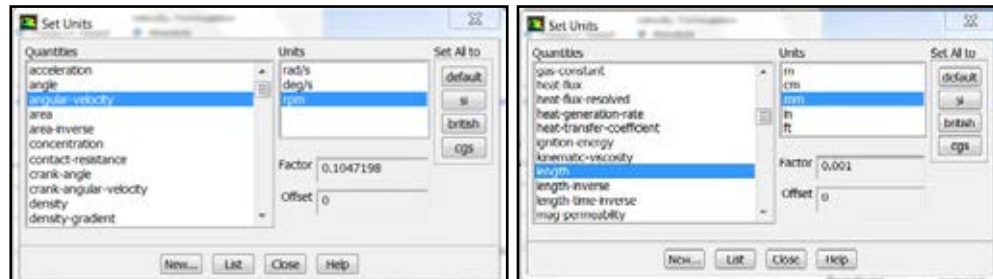
6. Check the domain whether it corresponded to actual physical dimension. Scale the mesh in millimeter unit.
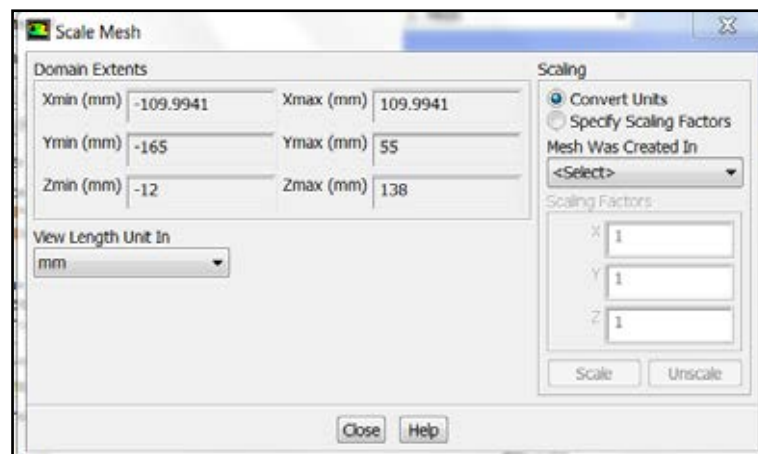
7. Next step, the **viscous model** was selected. Due to the mixing is in laminar flow, model panel was kept default.
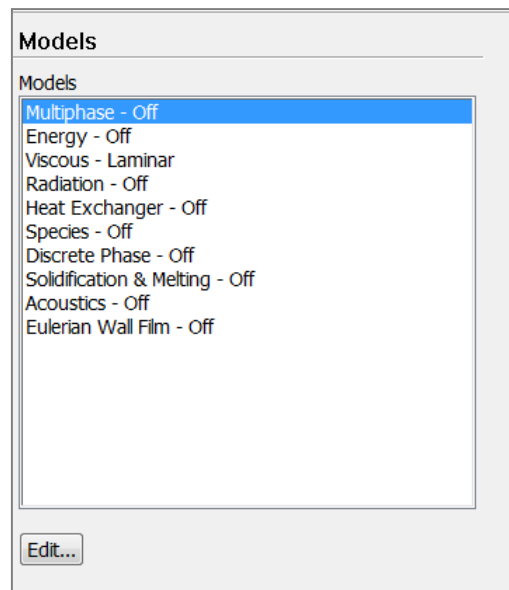
8. In material panel, added liquid water to the list of material. Click change/create to replace the existing data of air.

   Materials > Create/Edit > Fluent Fluid Material > Water liquid > Change/Create > Close
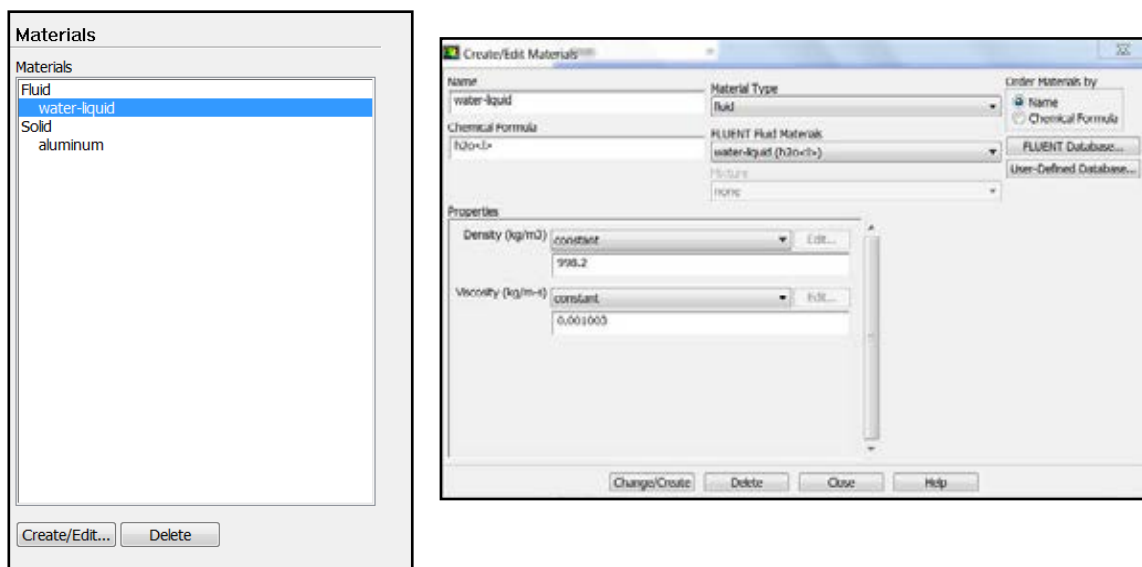
9. Define moving zone in **cell zone condition window** click **Edit**, frame motion and rotational velocity of 2000 rpm were selected.

Cell Zone Conditions > moving > Edit > OK
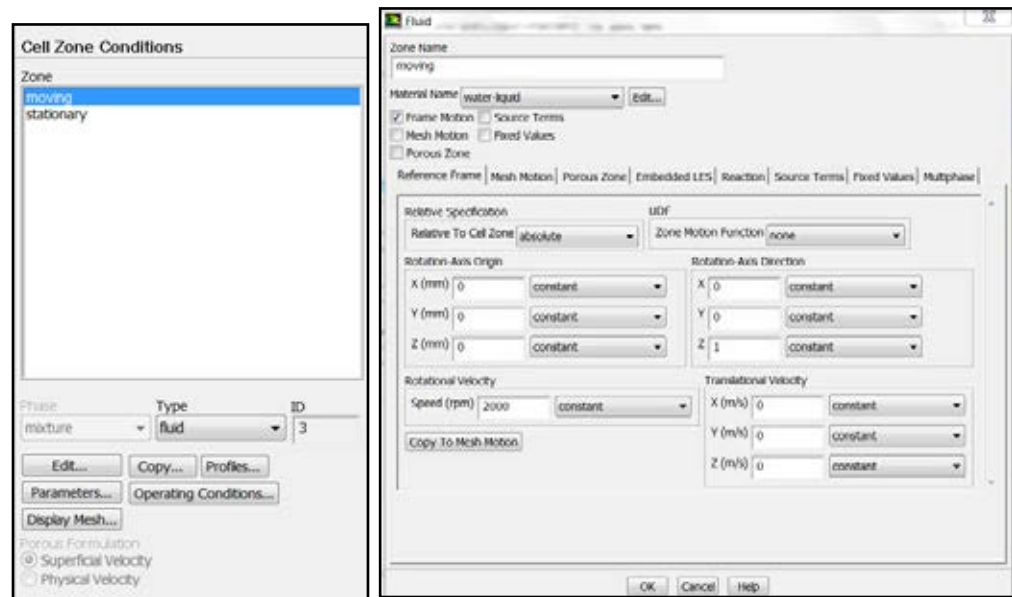
10. Kept default in **stationary zone**.
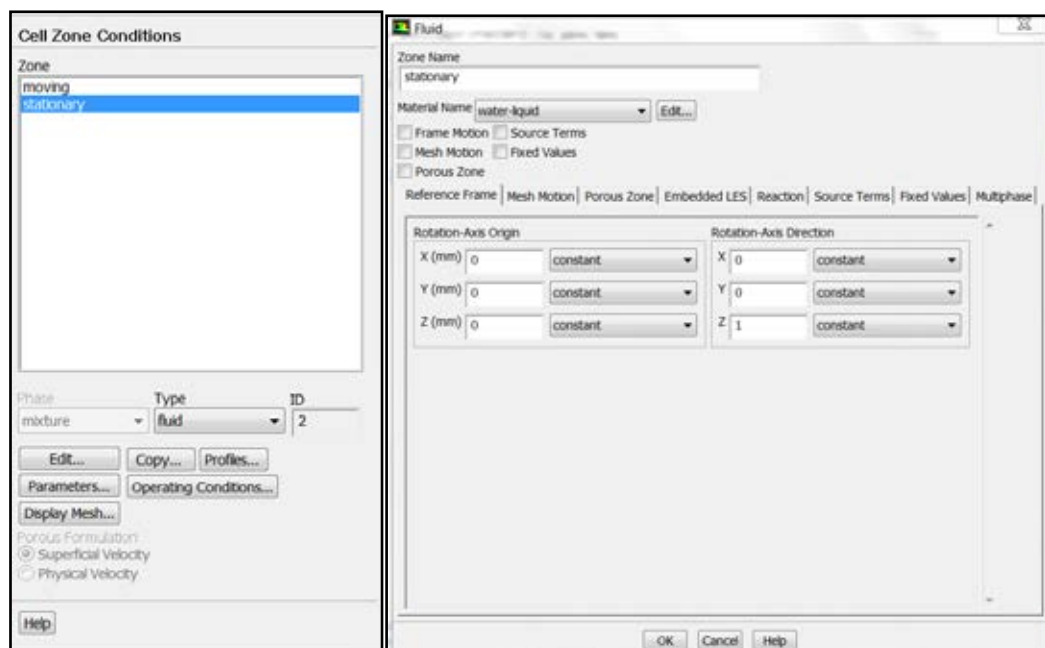
11. Define boundary conditions in **boundary condition window** click **Edit**.

- For **impeller boundary condition**, the **wall motion** was as stationary wall and **shear condition** was set as no slip.
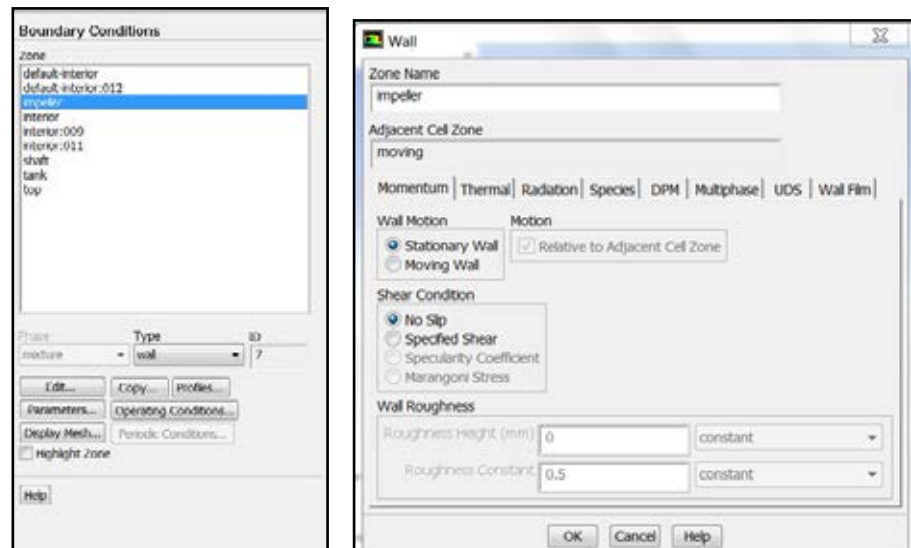

- For **shaft boundary** condition, the **wall motion** was as **moving** wall. **Motion** was set as absolute with rotational speed of 2000 rpm. Shear condition was set as no slip.
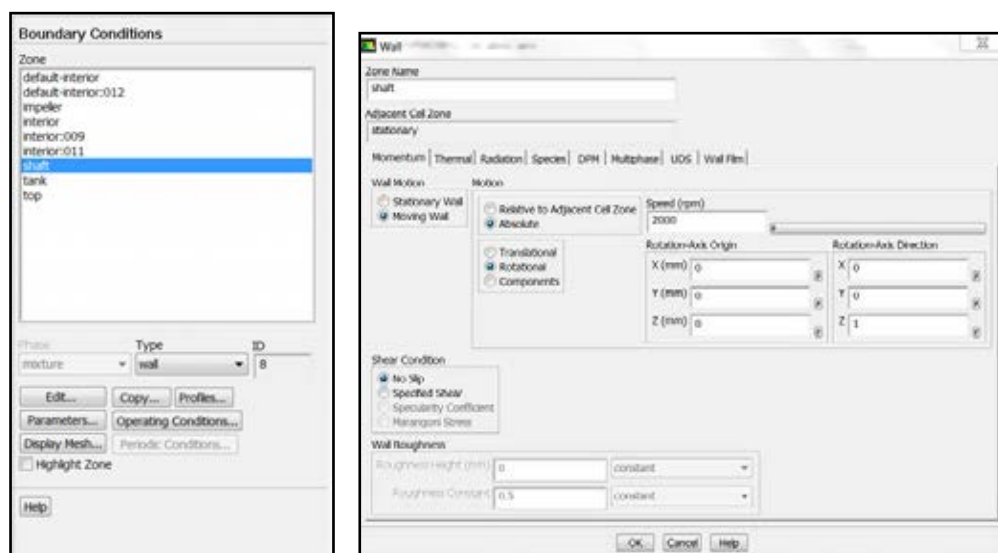
- For **tank boundary condition**, the **wall motion** was as stationary wall and **shear condition** was set as no slip.
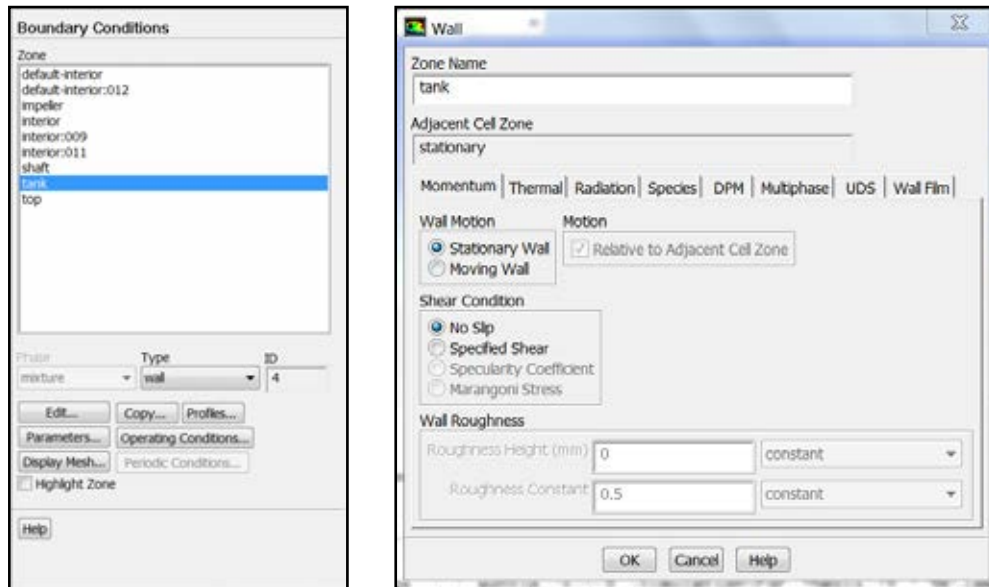
- For **top boundary condition**, the **wall motion** was as stationary wall and **shear condition** was set as no slip.
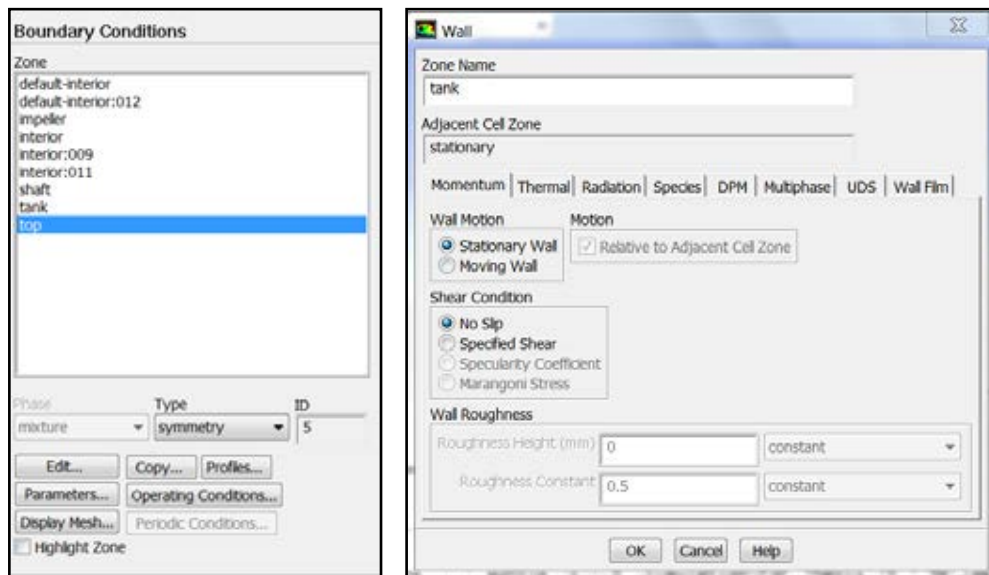
- The operating condition, **operating pressure** was set at 1 atm and gravity was kept default (as it was already set in scale setting step). The reference Pressure location was set at 138 mm in z position due to pressure acted on this location.

Define > Operating Conditions > OK
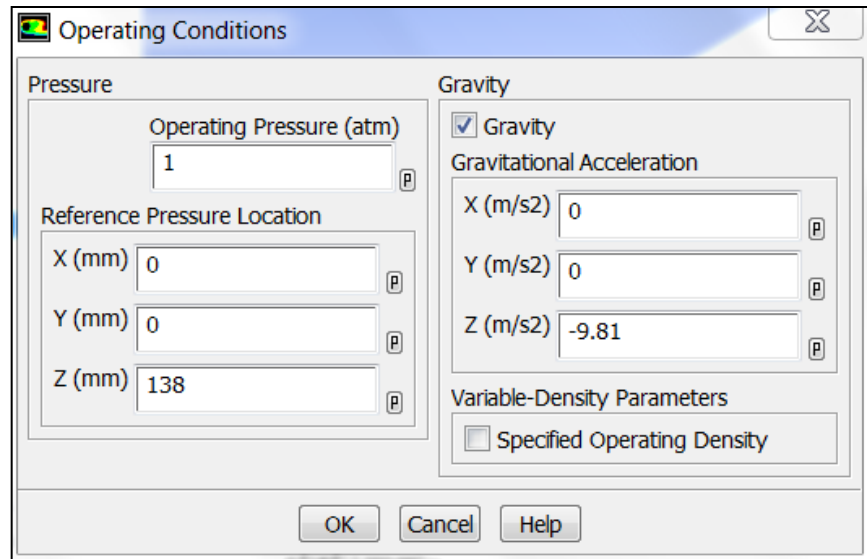
12. In **reference values** window, compute from panel was drop down and selected impeller. Area and length is impeller dimension. Density and viscosity are possessed by water. Reference zone was drop down and selected moving.
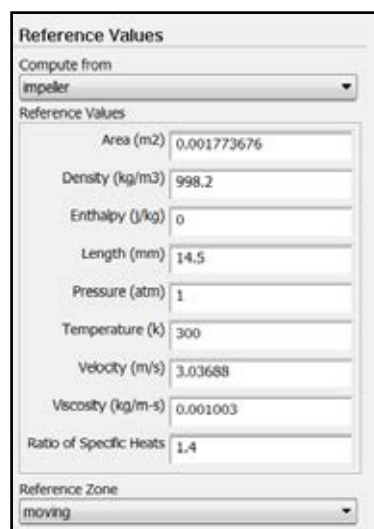
Step 2: Solution

1. In **solution methods** panel, the discretizations were defined as follows

Solve > Controls > Solution

Pressure-velocity coupling: Coupled
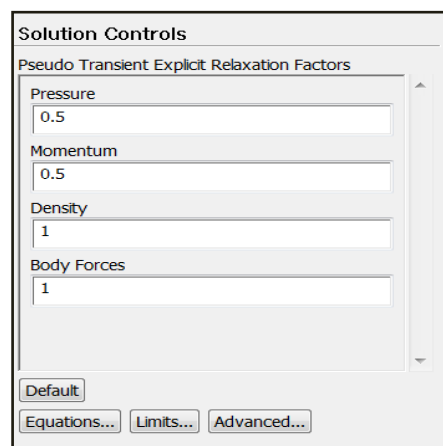
Gradient: Least Square Cell Based

Pressure: PRESTO

Momentum: First Order upwind

Pseudo Transient was enabled as recommended by FLUENT as it helped decrease number of iterations for convergence.
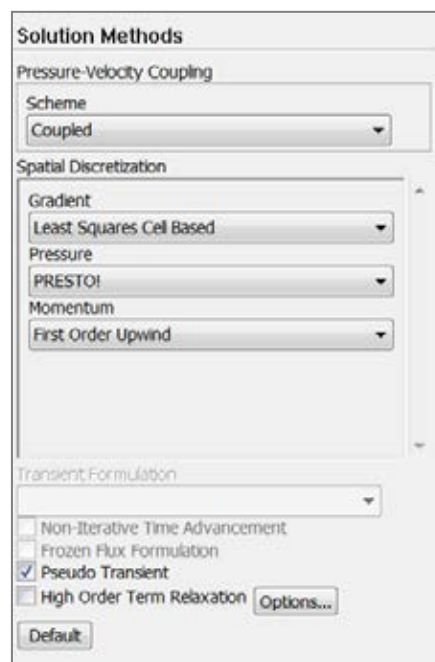
2. Retain the default **Control solution.**

3.

4. Initial the flow on **Solution initialization**. Select standard initialization and absolute reference frame.
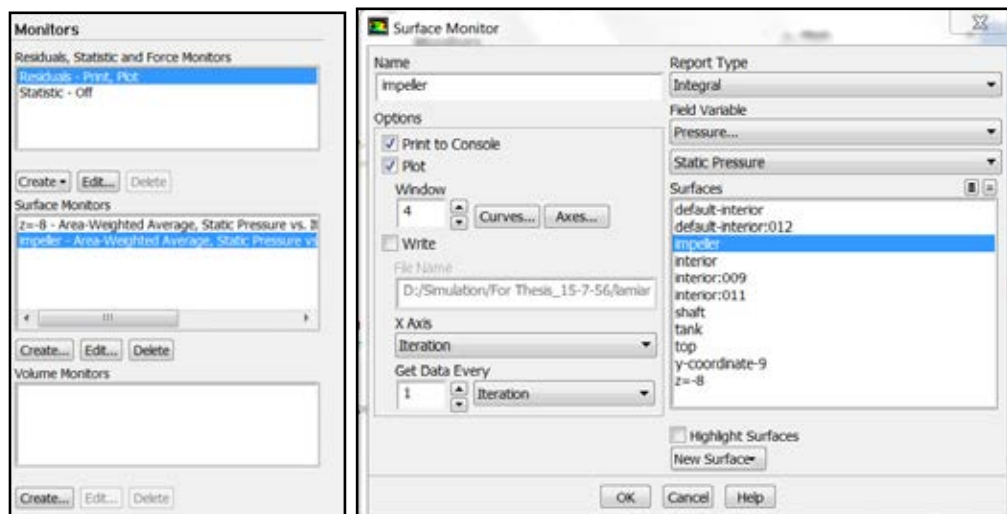
   Solution initialization > Initial
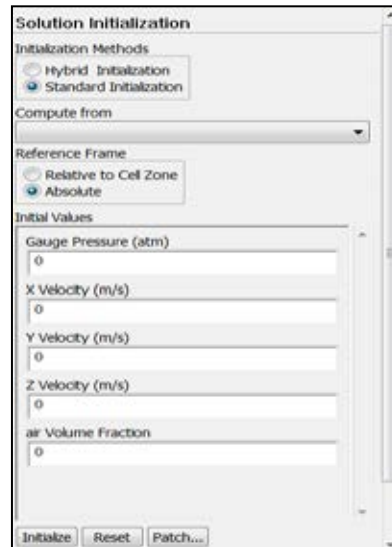
5. Create two new surfaces monitor. One monitor was to observed pressure along the impeller and the other one was to investigate velocity.
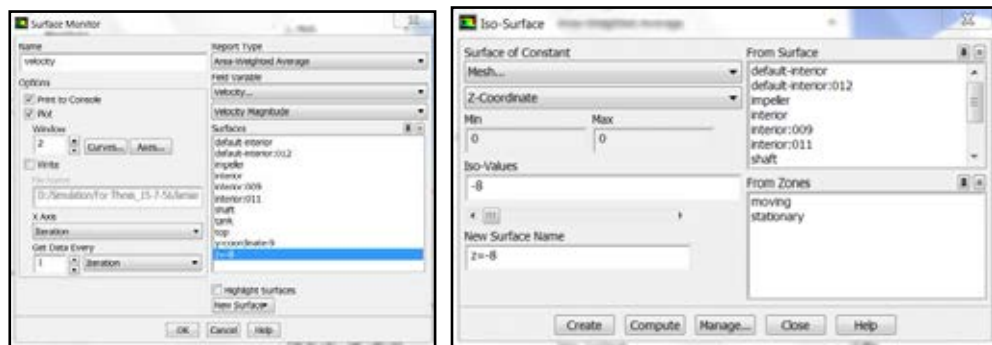
   Create pressure monitor

   - **Surface Monitors > Create > Surface > impeller >Name impeller > OK**

Create velocity monitor

- **Surface Monitors > Create > New Surface > Iso-Surface > Surface of Constant > z-coordinate > Iso-Values > New surface name z = -8**

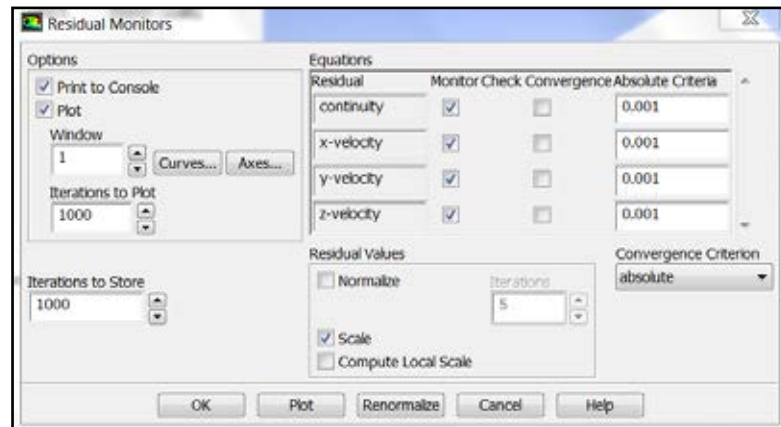6. Then, save case and data file.

   File > Write > Case (2000rpm_water)

7. Start the calculation by iterating the solution until the solution converges at 10^{-3} residue.

   Run Calculation > Calculate

8. After the solution are converged at 10^{-3} residuals, save case and data files (2000rpm_water.gz)

9. On the monitor panel, deselect convergence of residual plot for all equations.

   Click Plot >OK > Close

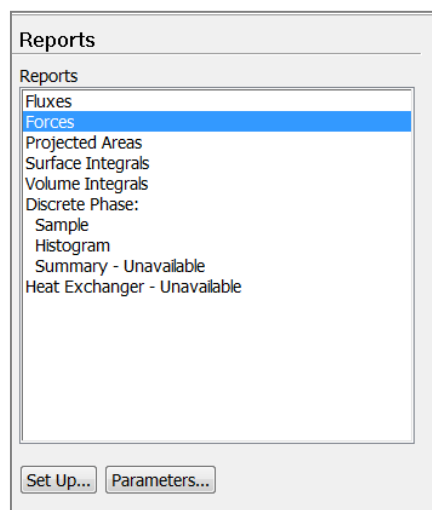10. Continue the calculation by iterating the solution until the monitors reached a constant value.

   Run Calculation > Calculate

11. Save case and data files (2000rpm_water.gz).
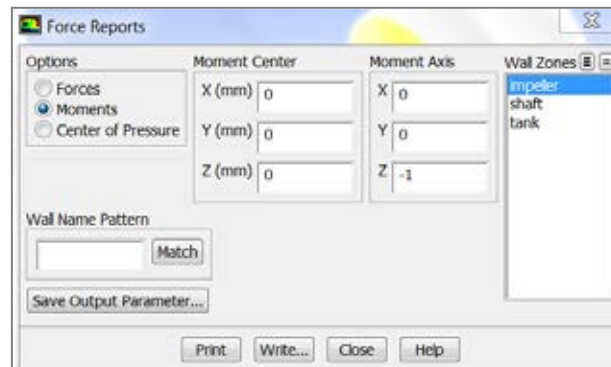
Step 3 Post-processing

1. This step torque calculation can be reported.

   Reports > Force > Force Report

2. In **force reports** panel**,** moments option was selected. Define the moment z-axis as -1 accordingly to vector moment direction. The summation of torque calculation acting on impeller was reported.

**Moments > add value -1 in Moment Axis > Print**

Variables input for FLUENT Multiphase (water-air)

Since the multiphase flow model of water-air was developed, the major specifications were similar to single phase. Minor differences were described in this section.

Step 1: Problem setup

1. The general settings were carried till the step of the viscous model. The multiphase model was added. Volume of Fluid (VOF) was selected. Number of Eulerian phase was kept constant at 2. Implicit scheme was selected. Retain the default settings

Models > Multiphase > Volume of Fluid
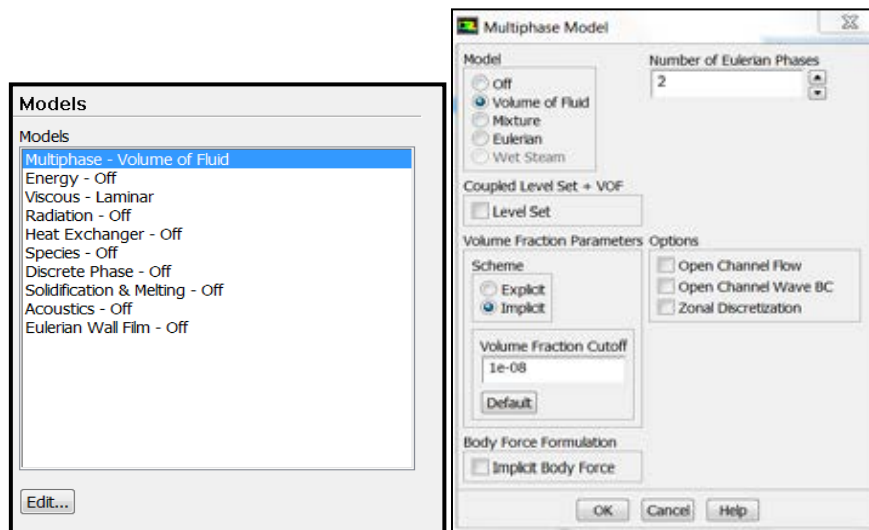
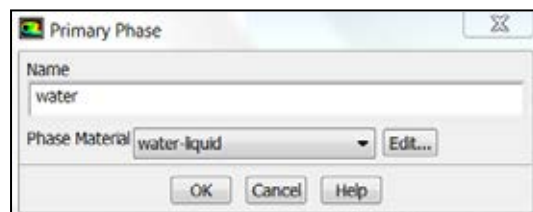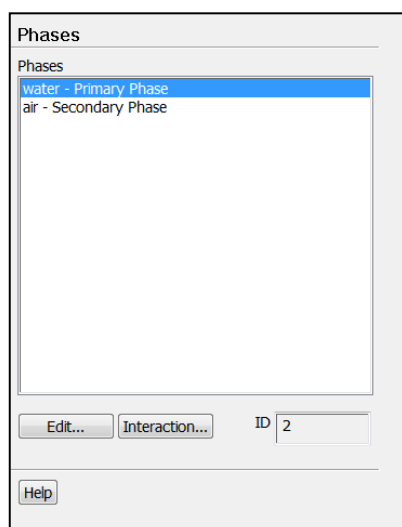2. Add water to the list of fluid material by keeping the existing data of air so that in material list consisted of water and air.
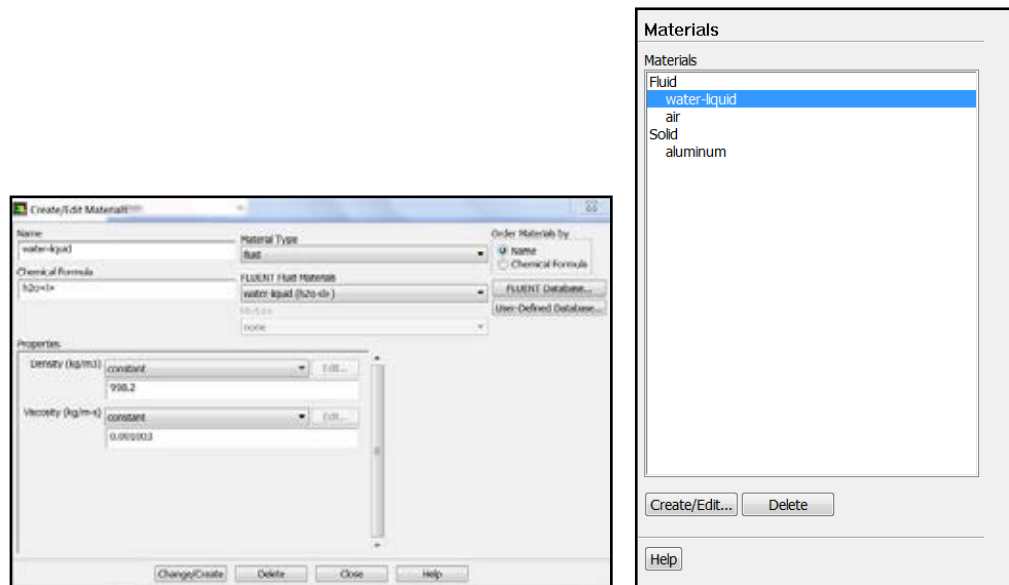
Materials > Create/Edit > Fluent Fluid Material > Water liquid > Change/Create > Close

3. The next step, specify the phases. Define water as primary phase where air was secondary phase.

Phases > Primary phase > Edit **>** Phase Material **>** Select Water
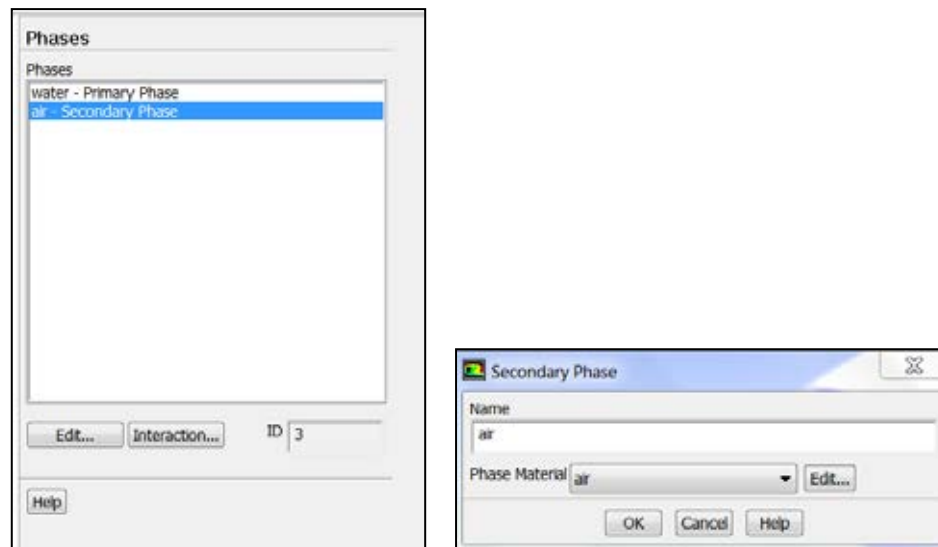
Secondary phase > Edit >Phase Material **>** Select Air

4. Define **cell zone condition** and **boundary condition** as the same procedure as single phase.

    Step 2: Solution

1. In **solution methods** panel, the discretizations were defined as follows

    Solve > Controls > Solution
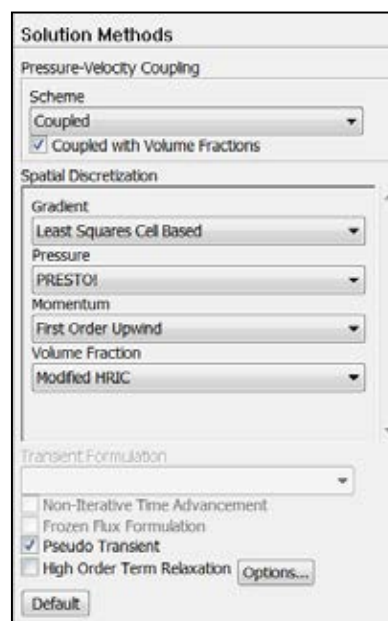
2. Retain the default **Control solution.**

      Pressure-velocity coupling: Coupled

      Gradient: Least Square Cell Based

      Pressure: PRESTO

      Momentum: First Order upwind

      Volume fraction: Modified HRIC

      Pseudo Transient was enabled as recommended by FLUENT as it helped decrease number of iterations for convergence.

3. Initial the flow on **Solution initialization**. Select standard initialization and absolute reference frame.

    Solution initialization > Initial
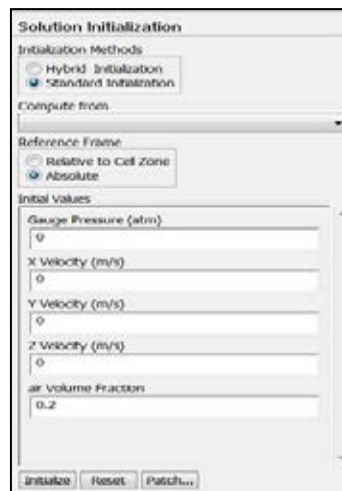
4. On the monitor panel, the same new surface monitors as single phase are created.

5. Define the starting height of the liquid inside the tank. On **region adaption** panel, the **input coordinate** in x, y, z positions are defined as follow.
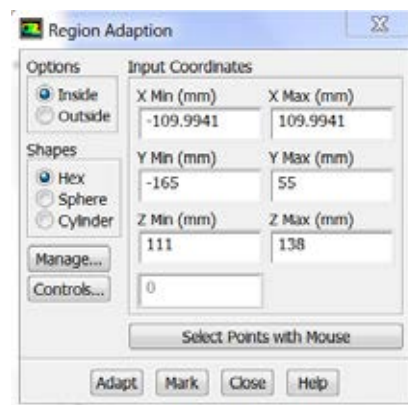
Adapt > Region > Region Adaption

Click > Mark

6. Then, save case and data file.

File > Write > Case (2000rpm_water_air)

7. Start the calculation by iterating the solution until the solution converges at 10^{-3} residue.

Run Calculation > Calculate

Run Calculation

Check Case...   Preview Mesh Motion...

Pseudo Transient Options

Fluid Zone

Time Step Method   Timescale Factor
○ User Specified   1
● Automatic

Length Scale Method   Verbosity
Conservative   ▼   0

Number of Iterations   Reporting Interval
3000   1

Profile Update Interval
1

Data File Quantities...   Acoustic Signals...

Calculate

8. After the solution are converged at 10^{-3} residuals, save case and data files (2000rpm_water.gz).
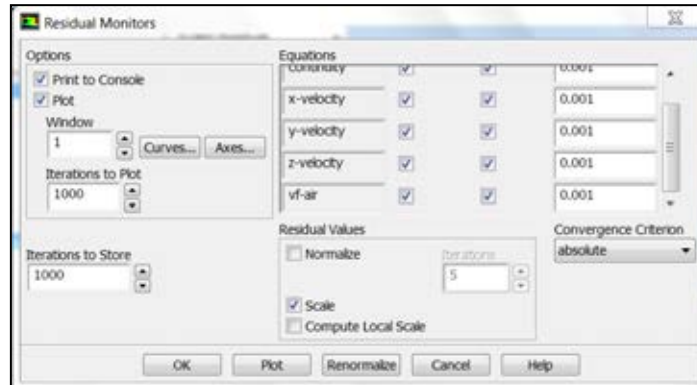
12. On the monitor panel, deselect convergence of residual plot for all equations.

   Click Plot >OK > Close

Residual Monitors

Options
☑ Print to Console
☑ Plot
Window
1   Curves... Axes...
Iterations to Plot
1000

Iterations to Store
1000

Equations
continuity   ☑   ☑   0.001
x-velocity   ☑   ☑   0.001
y-velocity   ☑   ☑   0.001
z-velocity   ☑   ☑   0.001
vf-air   ☑   ☑   0.001

Residual Values   Convergence Criterion
☐ Normalize   absolute   ▼
                    Iterations
                    5
☑ Scale
☐ Compute Local Scale

OK   Plot   Renormalize   Cancel   Help

13. Continue the calculation by iterating the solution until the monitors reached a constant value.

   Run Calculation > Calculate

14. Save case and data files (2000rpm_water_air.gz).

Step 3 Post-processing

The torque calculation step can be followed the single phase reporting.

APPENDIX B

STATISTIC CALCULATION

❖ **Deviation**

Speed (rpm)	2000	2100	2200	2300	2400	2500	2600	2700	2800	2900
Experiment I	24.396	24.852	25.308	26.106	26.904	27.930	29.298	33.288	37.392	39.672
Experiment II	23.422	23.991	24.559	25.241	26.151	27.174	29.298	33.288	35.929	38.772
$\bar{x}$	23.91	24.42	24.93	25.67	26.53	27.55	29.30	33.29	36.66	39.22
s	0.69	0.61	0.53	0.61	0.53	0.53	0.00	0.00	1.03	0.64
RSD	2.9	2.5	2.1	2.4	2.0	1.9	0.0	0.0	2.8	1.6

Average ($\bar{x}$)

$$\bar{x} = \frac{x_1 + x_2 + x_3 + x_4 + ...}{n}$$

Standard Deviation (s)

$$s = \sqrt{\frac{(x_1 - \bar{x})^2 + (x_2 - \bar{x})^2 + (x_3 - \bar{x})^2 + ...}{n - 1}}$$

Relative Standard Deviation (RSD) $RSD = (s/\bar{x}) \times 100$

❖ **Percent error**

Error = (Expt Value – Predicted Value) X 100

Expt Value

BIOGRAPHY

Miss Nantikan Lamaipan was born in September 25 th, 1987 in Bangkok, Thailand. She graduated in Bachelor's degree from the department of Chemical Technology, Chulalongkorn University in May 2010. Then, she has studied further in the Master's Degree from department of Chemical Engineering, Chulalongkorn University and has joined the Biochemical Engineering Research Laboratory since in 2010.

In April 2013, she participated in PPC Symposium on Petroleum, Petrochemical and Polymers Conference (PEREOMAT and PPC SYM 2013), Bangkok, Thailand for proceeding published in "Computational Fluid Dynamics modeling of a mixing tank for the production of shellac-carnauba wax fruit coating solution".